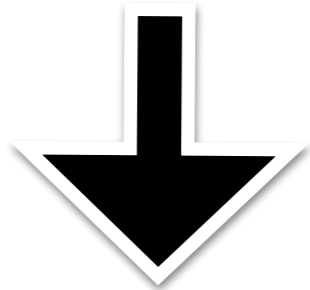


# MSP BINARIES: PROBES OF RELATIVISTIC SHOCK ACCELERATION AND PULSAR WINDS

Zorawar Wadiasingh (CSR NWU)  
Alice K. Harding (NASA GSFC)  
Christo Venter (CSR NWU)  
Markus Böttcher (CSR NWU)

# Black Widows & Redbacks



Nearly all *circular* orbits

Table 1. Measured and derived parameters of BW pulsars.

Name	$P_{\text{ms}}$	$\dot{P}_i$ ( $10^{-20}$ )	$L_{\text{sd}}^{\text{a}}$ ( $10^{34} \text{ erg s}^{-1}$ )	$B_{\text{s}}^{\text{b}}$	$d$ (kpc)	$P_{\text{b}}$ (h)	$M_{\text{comp}}$ ( $M_{\odot}$ )	$a_{11}$	$E_{\text{cut}}$ (TeV)	Ref.
J0023+0923 <sup>c</sup>	3.05	1.15	2.50	4.88	0.7	3.3	0.016	1.01	2.40	1
J0610–2100 <sup>c</sup>	3.86	0.34	0.36	2.96	3.5	6.9	0.025	1.65	3.04	2
J1124–3653 <sup>c</sup>	2.41	0.57	2.50	3.05	1.7	5.4	0.027	1.40	2.03	1
J1301+0833 <sup>c</sup>	1.84	0.95	9.36	3.44	0.7	6.5	0.024	1.59	1.37	3
J1311–3430 <sup>c</sup>	2.56	2.08	7.64	6.01	1.4	1.56	0.008	0.61	2.33	4
J1446–4701 <sup>c</sup>	2.19	1.01	5.93	3.88	1.5	6.7	0.019	1.62	1.52	5
J1544+4937 <sup>c</sup>	2.16	0.31	1.87	2.12	1.2	2.8	0.018	0.91	2.72	6
J1731–1847	2.34	2.47	11.9	6.26	2.5	7.5	0.04	1.75	1.23	7
J1745+1017 <sup>c</sup>	2.65	0.23	0.75	2.02	1.36	17.5	0.016	3.07	1.86	8
J1810+1744 <sup>c</sup>	1.66	0.45	6.08	2.26	2	3.6	0.044	1.07	1.86	1
J1959+2048 <sup>c</sup>	1.61	0.72	10.6	2.80	1.53	9.2	0.021	2.00	1.19	9
J2047+1053 <sup>c</sup>	4.29	2.00	1.56	7.63	2	3	0.035	0.95	2.78	3
J2051–0827 <sup>c</sup>	4.51	1.23	0.83	6.14	1	2.4	0.027	0.82	3.51	2
J2214+3000 <sup>c</sup>	3.12	1.46	2.96	5.57	1.32	10	0.014	2.11	1.59	10, 11
J2234+0944 <sup>c</sup>	3.63	1.94	2.50	6.91	1	10	0.015	2.11	1.66	3, 5
J2241–5236 <sup>c</sup>	2.19	0.67	3.90	3.15	0.5	3.4	0.012	1.03	2.12	12
J2256–1024 <sup>c</sup>	2.29	1.58	8.11	4.96	0.6	5.1	0.034	1.35	1.54	1

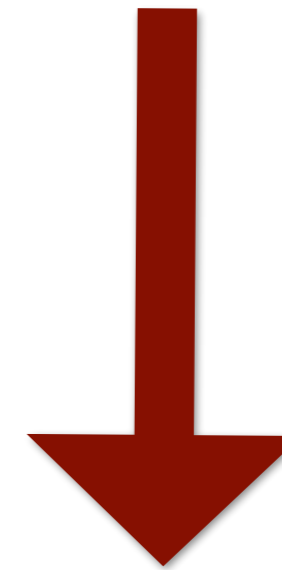


Table 2. Measured and derived parameters of RB pulsars.

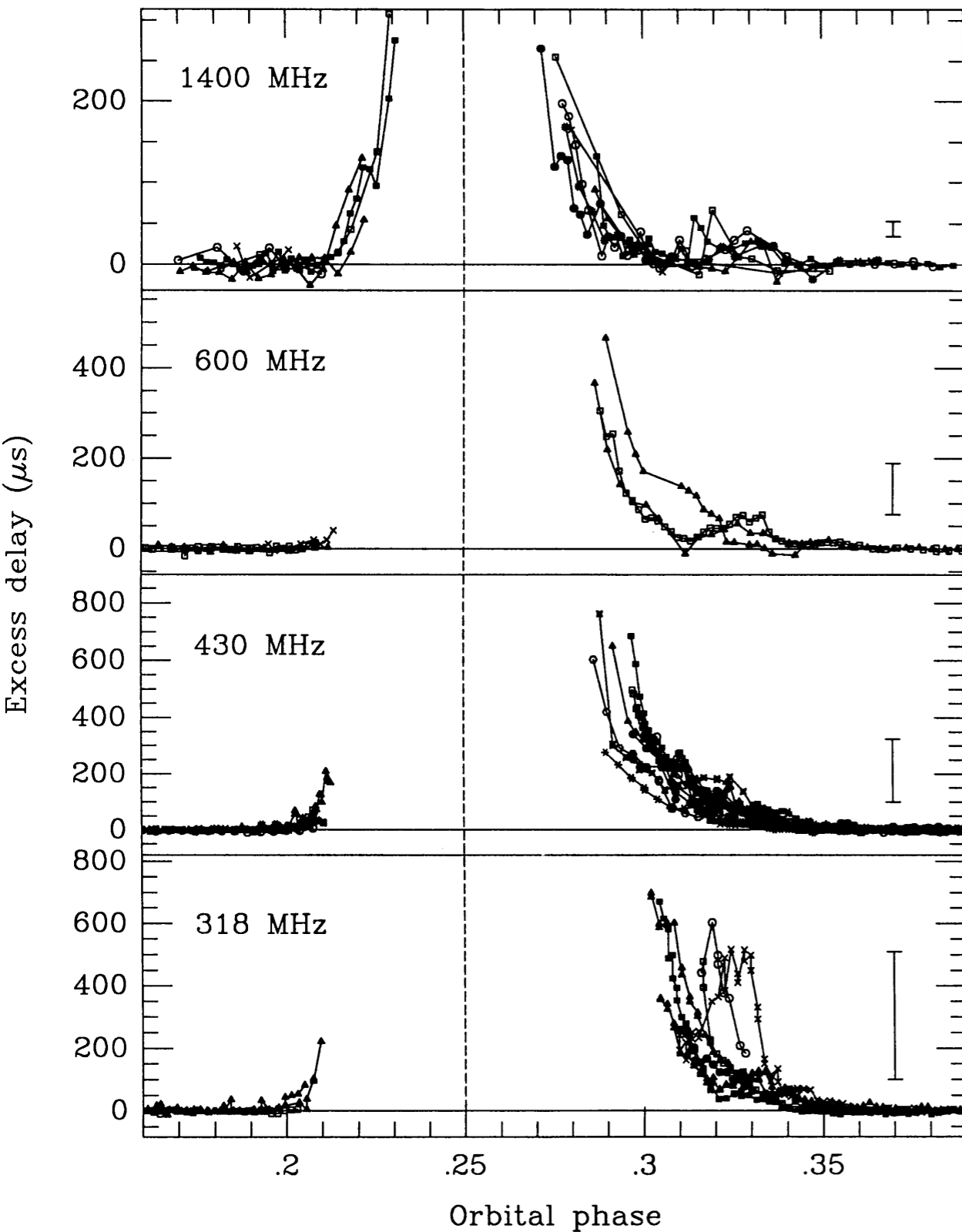
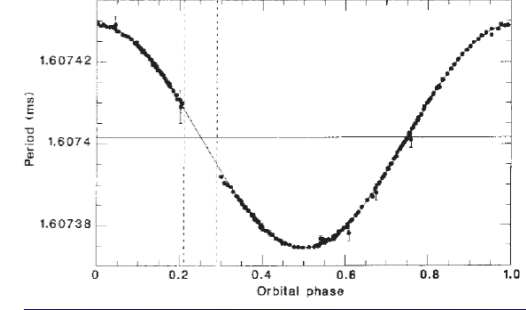
Name	$P_{\text{ms}}$	$\dot{P}_i$ ( $10^{-20}$ )	$L_{\text{sd}}^{\text{a}}$ ( $10^{34} \text{ erg s}^{-1}$ )	$B_{\text{s}}^{\text{b}}$	$d$ (kpc)	$P_{\text{b}}$ (h)	$M_{\text{comp}}$ ( $M_{\odot}$ )	$a_{11}$	$E_{\text{cut}}$ (TeV)	Ref.
J1023+0038	1.69	1.20	15.4	3.72	0.6	4.8	0.2	1.33	1.33	1
J1628–3205	3.21	1.13	2.11	4.96	1.2	5	0.16	1.36	2.15	2
J1723–2837	1.86	0.75	7.18	3.08	0.75	14.8	0.4	2.90	1.09	3, 4
J1816+4510 <sup>c</sup>	3.19	4.03	7.64	9.34	2.4	8.7	0.16	1.97	1.30	5
J2129–0429	7.61	43.54	6.08	47.4	0.9	15.2	0.37	2.94	1.12	6
J2215+5135 <sup>c</sup>	2.61	2.79	9.67	7.03	3	4.2	0.22	1.22	1.55	6
J2339–0533 <sup>c</sup>	2.88	1.39	3.59	5.21	0.4	4.6	0.26	1.30	1.93	7, 8

Venter et al. (2015)

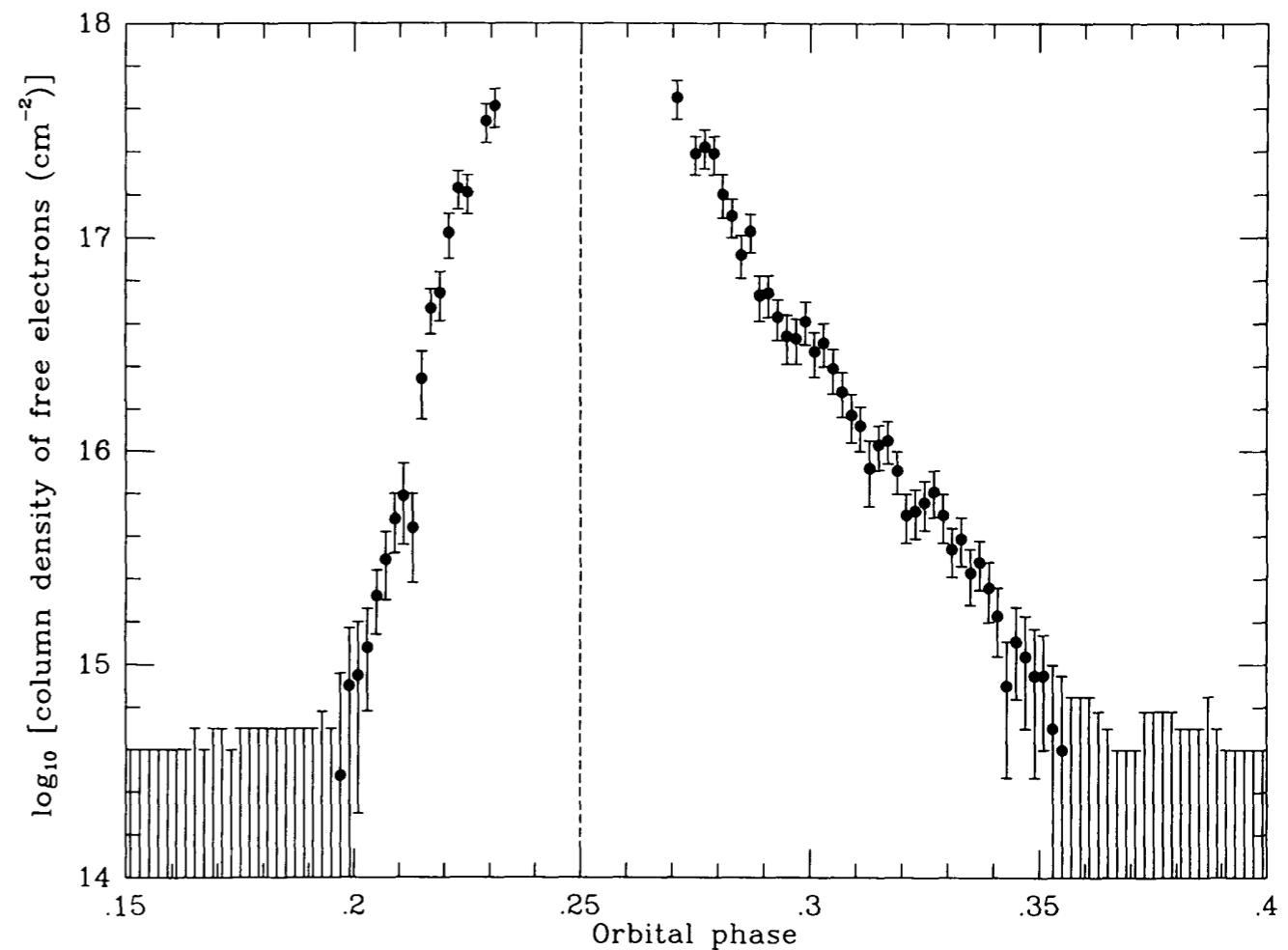
Much of *this* talk is focused on **B1957+20/J1959+2048**, the *original* Black Widow, but the methods developed here will be applied to more of these systems in the near future



# Radio Eclipses



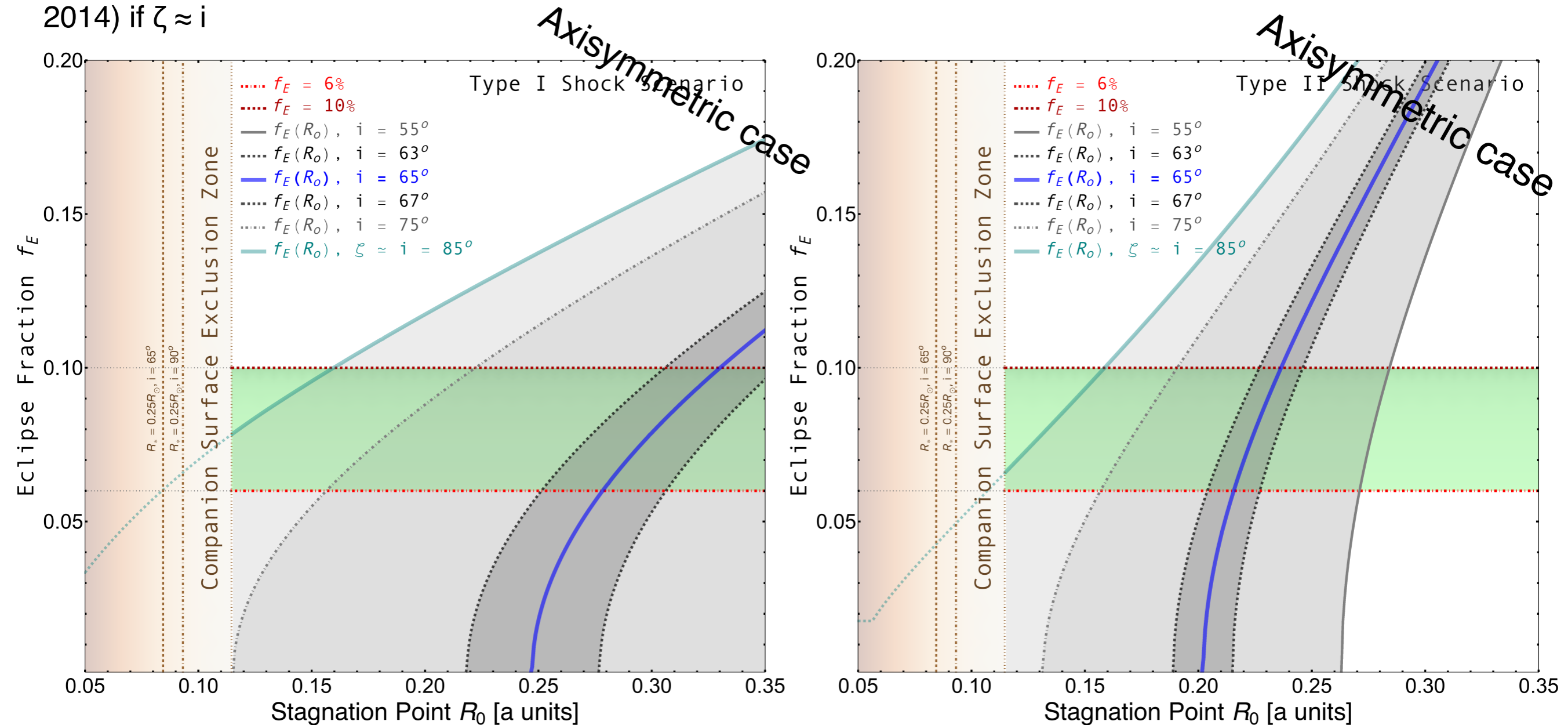
- Many black widows and redbacks show frequency-dependent **radio eclipses or shrouding** of the MSP over large fractions of their orbit, centered at superior conjunction where the companion is between the observer and MSP
- Ingress-egress shrouding asymmetry tends to always decrease with higher observing frequencies ==> high frequencies probe denser wind regions closer to the shock where asymmetry due to orbital motion is lower



Ryba & Taylor (1991) — B1957+20

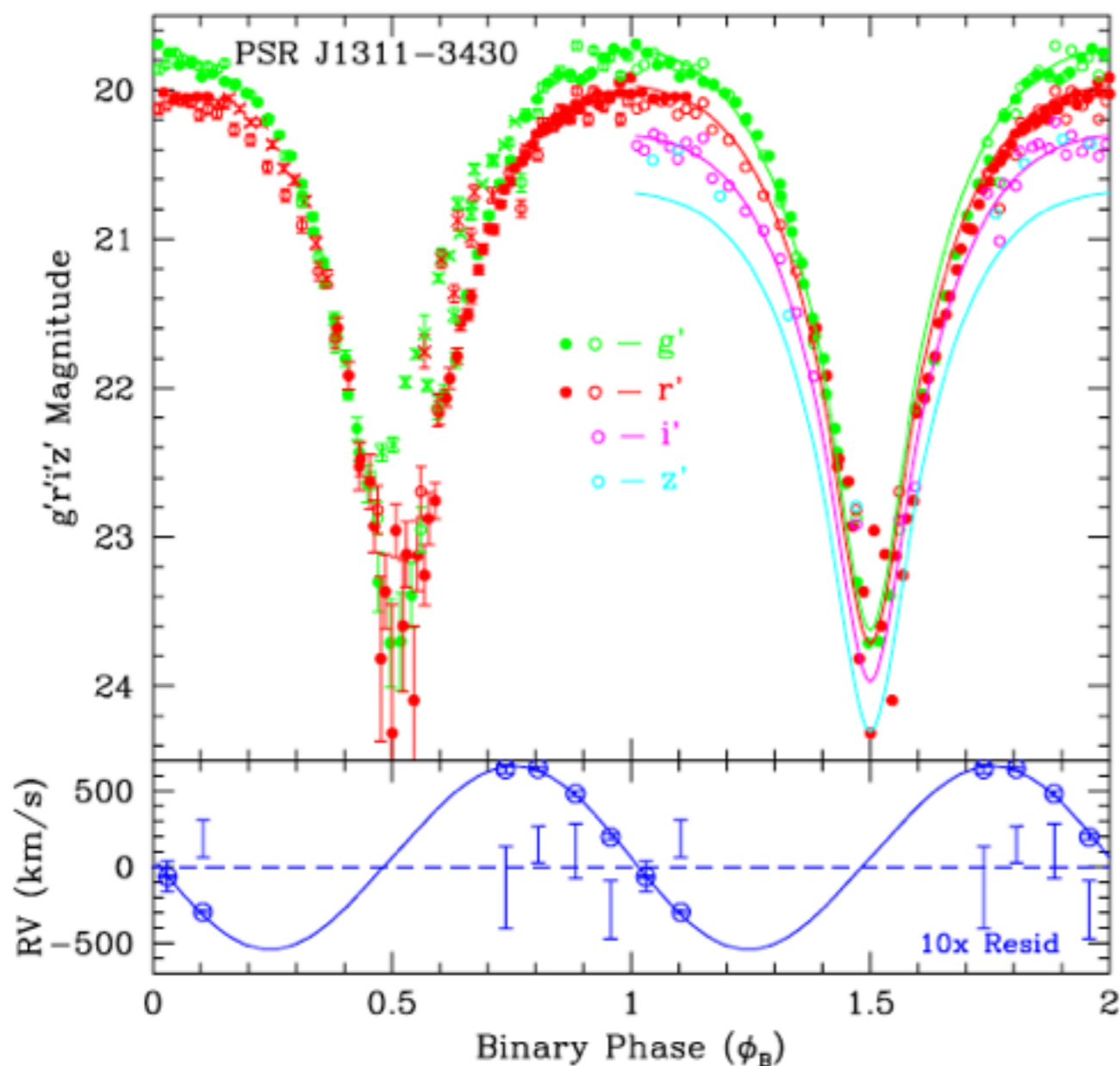
# Estimating Shock Containment & Inclination with Radio Eclipses

- We model two types of bow shocks, a "type I" parallel-wind (Wilkin 1996) and "type II" two-spherical-wind shock (Canto et al. 1996) and adopt an optically thick model for eclipses (Rasio et al. 1989)
- One-to-one coupling between eclipse fraction and orbital inclination  $i$  for a shock with stand-off distance  $R_0 - R_0$  values compatible with kilogauss companion magnetospheres or thermally driven winds
- B1957+20: 6-10% eclipse fraction (green band)
- Blue line:  $65^\circ \pm 2^\circ$  (Reynolds et al. 2007) with looser limits  $55^\circ$ - $75^\circ$  (van Kerkwijk et al. 2011)
- Cyan line:  $i \approx 85^\circ$  found from outer-magnetospheric pulsed  $\gamma$ -ray light curve modeling of the MSP (Johnson et al. 2014) if  $\zeta \approx i$

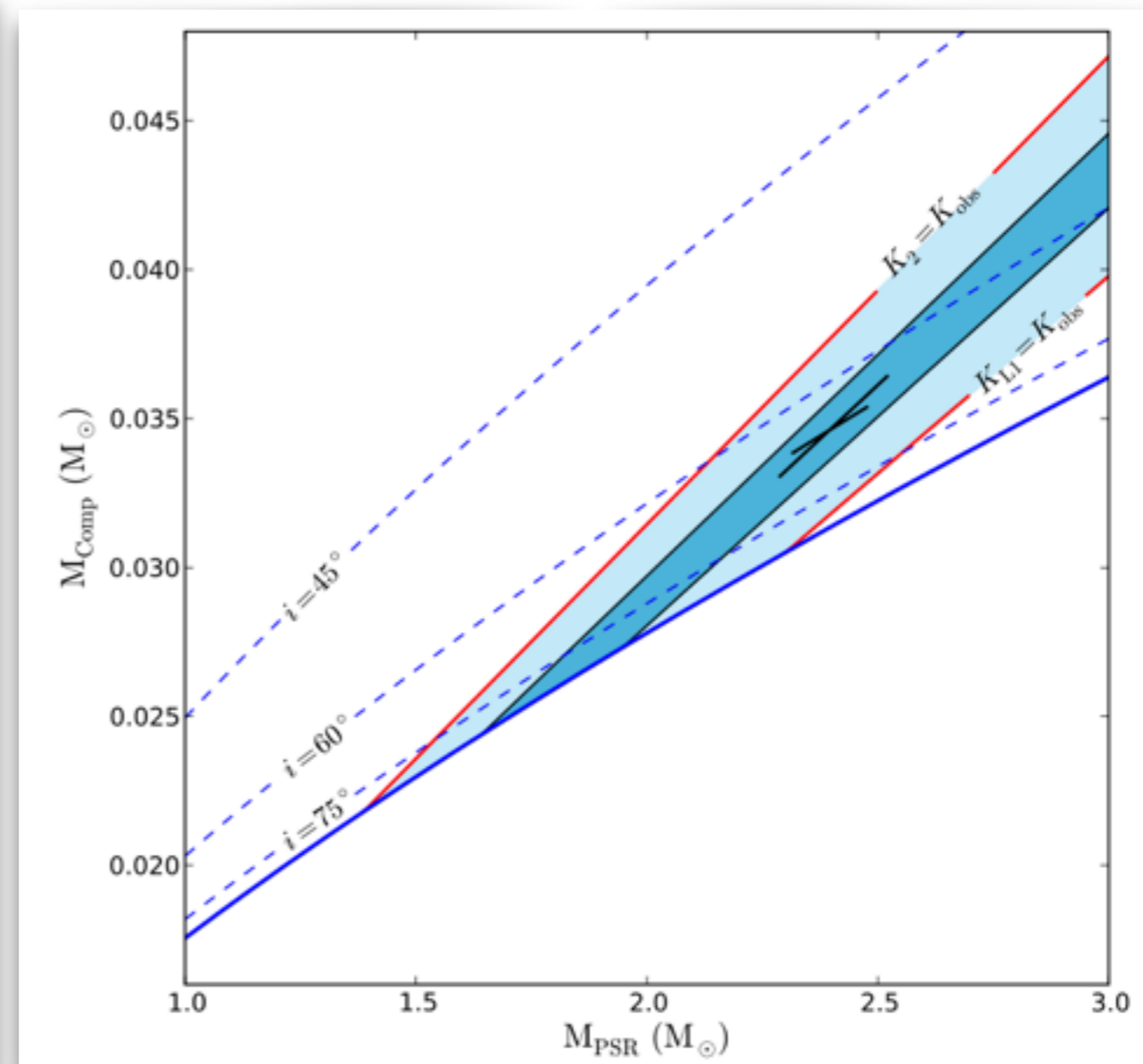


# Optical Observations of the Stellar Companion

- Photometry with a model of anisotropic heating can constrain the system inclination
- Spectroscopic radial velocity studies can constrain the mass ratio
- Companion temperature as high as few times  $10^4$  K on heated side



J1311-3430, Romani et al. (2012)

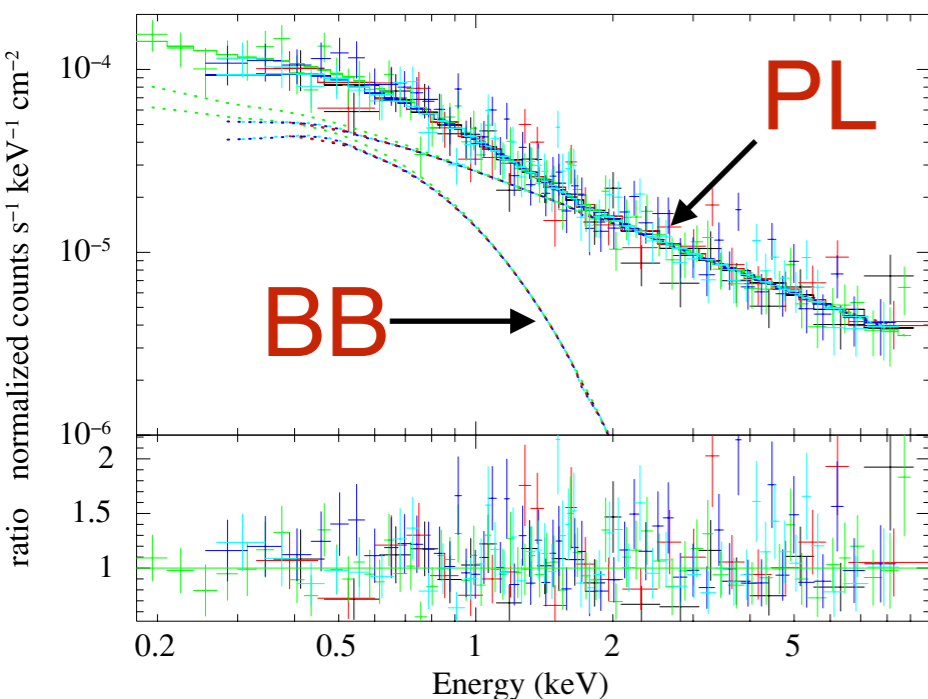


B1957+20, van Kerkwijk et al. (2011)

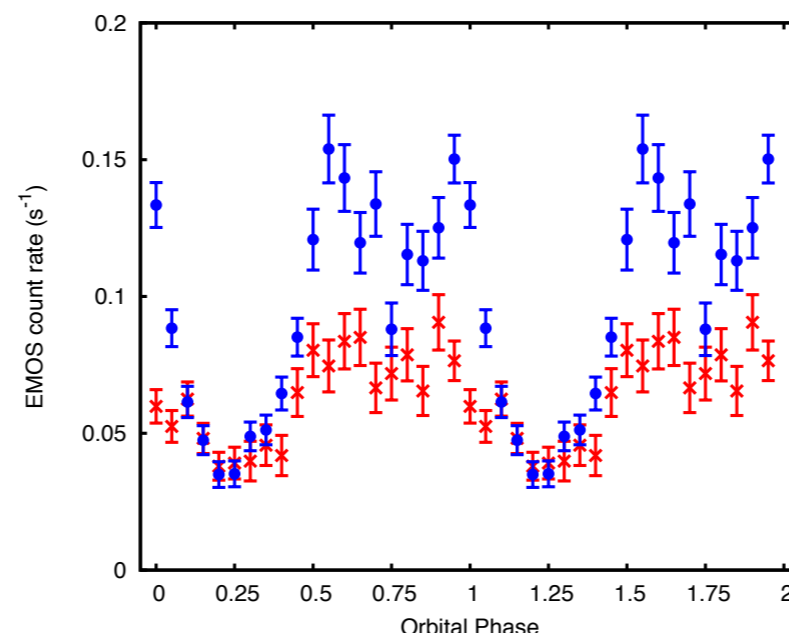
# X-ray Observations

- Soft X-ray observations of many black widows and redbacks show a flux minimum around superior or inferior conjunction, and many exhibit double-peaked light curves
- The emission is likely due to synchrotron radiation, modulation by Doppler boosting and/or shadowing by the companion
- Spectral photon indices are typically  $\Gamma \approx 1-1.5$  implying very hard underlying electron power-law distributions and efficient acceleration

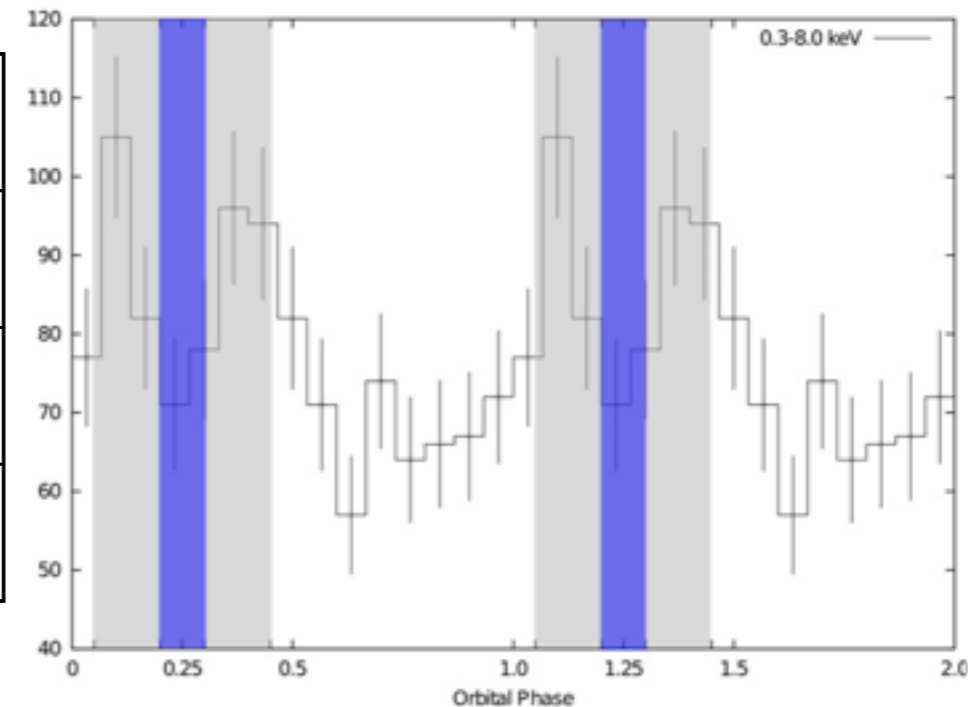
J1023+0038 (rotation-powered state)  
Archibald et al. (2010)



J1227-4853, de Martino et al. (2015)

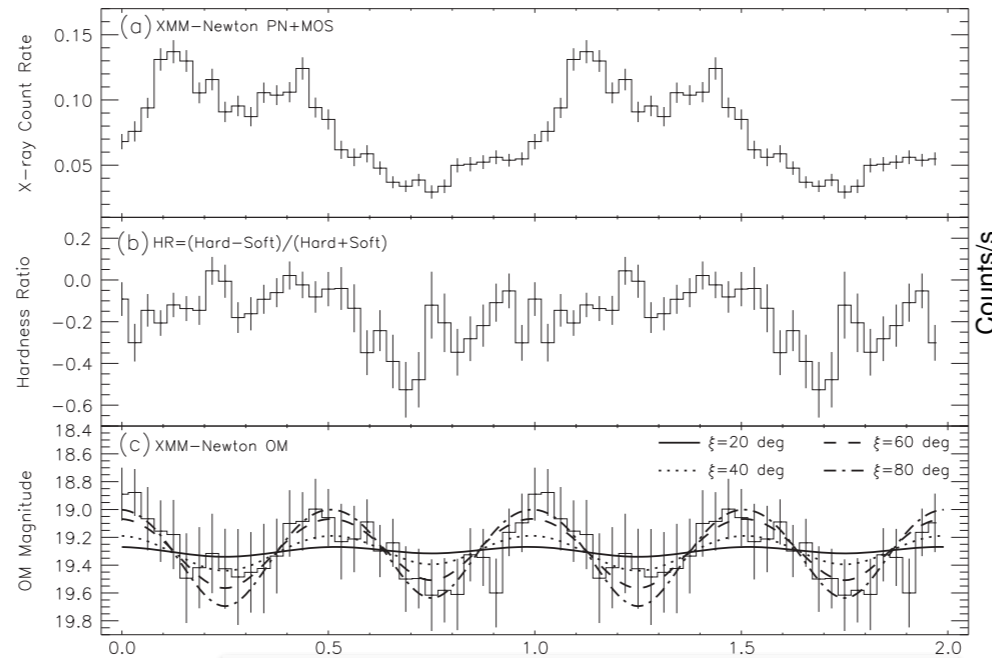


B1957+20, Huang et al. (2012)

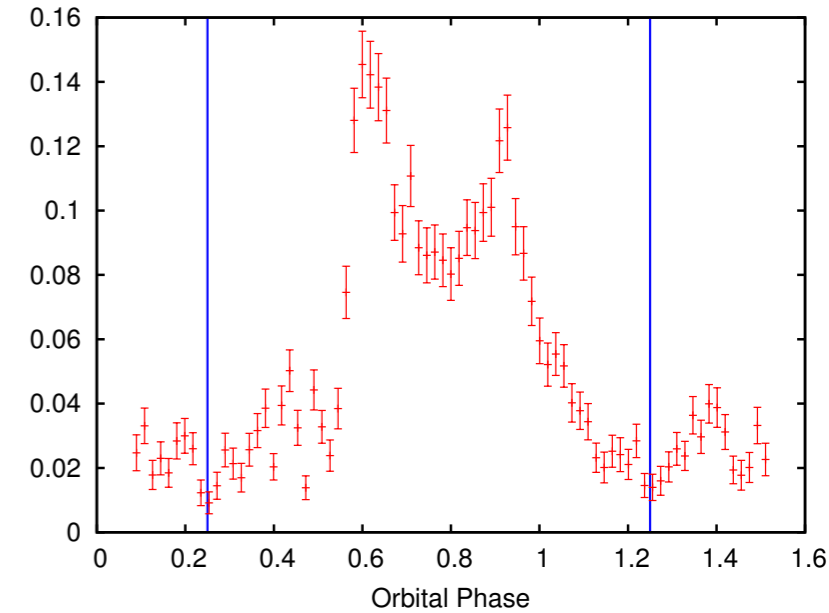


# Double-Peaked Soft X-ray Light Curves

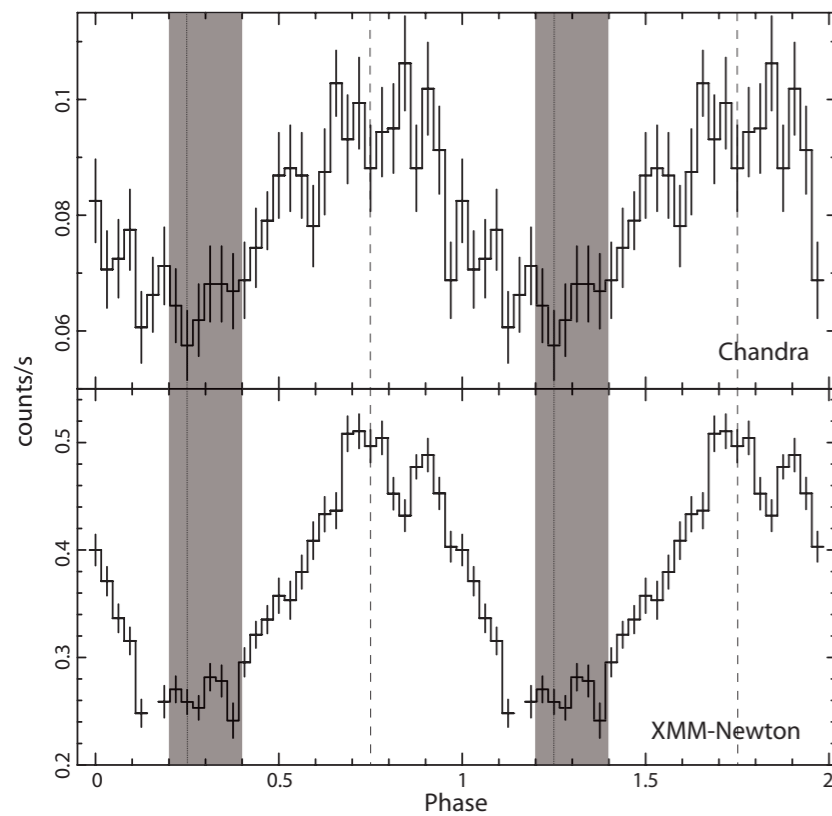
- Centered about inferior or superior conjunction
- Second peak nearly always at a modestly lower flux level



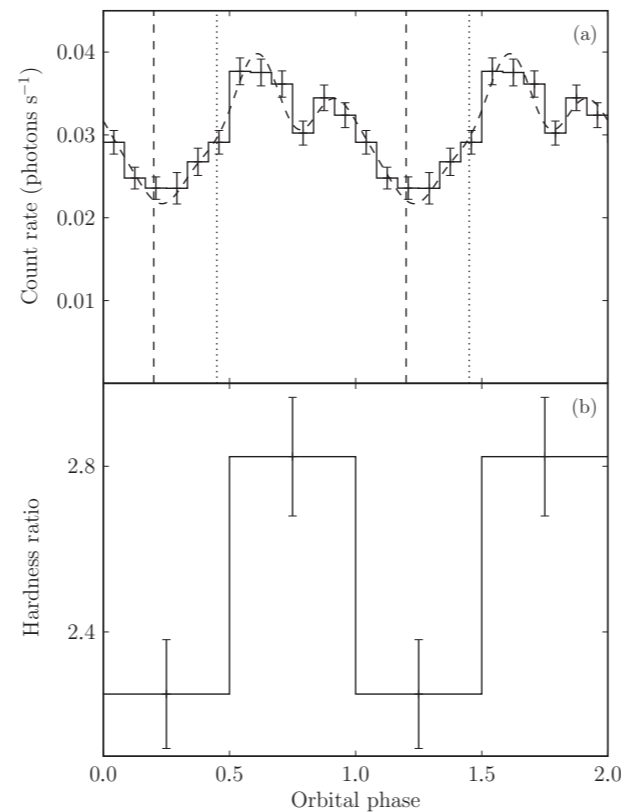
**J2129-0429, Hui et al. (2015)**



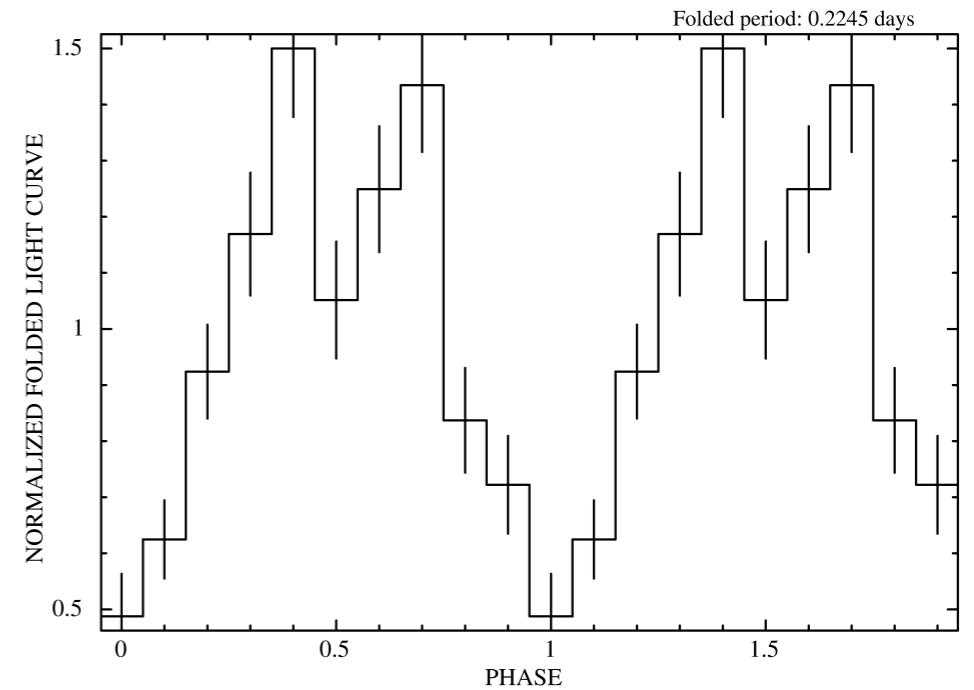
**J2129-0429, Roberts et al. (2015)**



**J1723-2837, Hui et al. (2014)**



**J1023+0038, Archibald et al. (2010)**



**J2039-5618, Salvetti et al. (2015)**

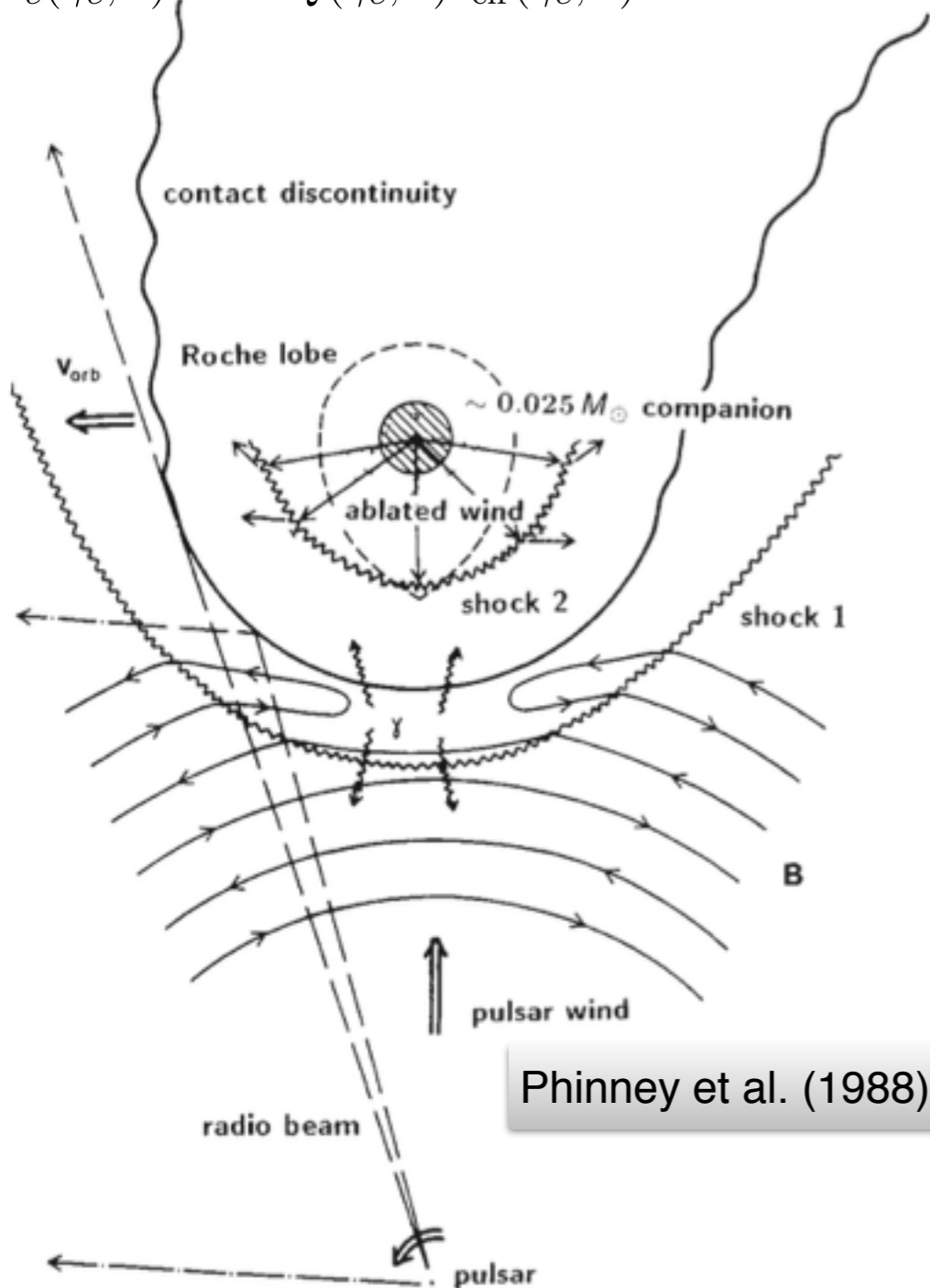


# Particle Acceleration

Shock is only  $\sim 10^{11}$  cm away from the MSP in black widows, contrasted to  $\sim 10^{15}-10^{17}$  cm for PWNe

$$\tau_{\text{eff}} = \left[ \frac{1}{\tau_{\mathcal{D}}} + \frac{1}{\tau_{\text{conv}}} + \frac{1}{\tau_{\text{ad}}} + \frac{1}{\tau_{\text{rad}}} + \frac{1}{\tau_{\text{cat}}} \right]^{-1}$$

$$n_e(\gamma_e, \theta) \sim Q(\gamma_e, \theta) \tau_{\text{eff}}(\gamma_e, \theta).$$



## Shock acceleration spectrum

$$N_p(E) = Q_0 E^{-2} \exp(-E / E_{\text{max}})$$

## Maximum acceleration energy (Harding & Gaissner 1990)

$$E_{\text{max}} = 2.6 \text{ TeV } B_8^{-1/2} P_{ms} a_{11}^{-1/2} \left( \frac{a}{r_s} \right)^{1/2} \sqrt{\frac{3(\xi - 1)}{\xi(\xi + 1)}}$$

## Normalization

$$\int_{E_{\text{min}}}^{\infty} N_p(E) dE = M_+ \dot{n}_{GJ}$$

Pair multiplicity

$$\int_{E_{\text{min}}}^{\infty} N_p(E) E dE = \eta_p \dot{E}$$

Efficiency

Polar cap flux

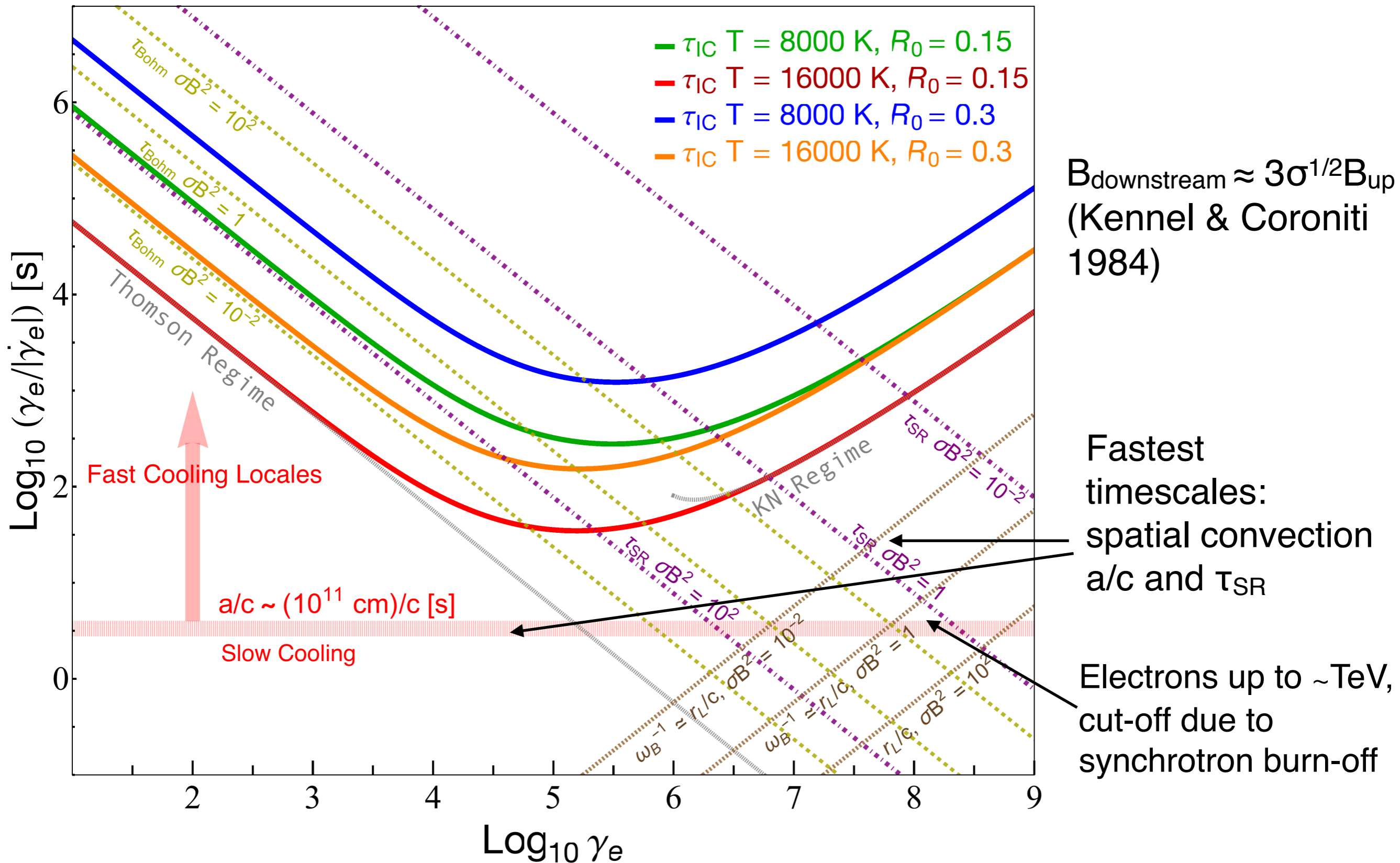
The shock is quasi-perpendicular, relativistic and possibly magnetically dominated  $\sigma \gg 1$  upstream — reconnection or DSA?

Emission & particle cooling should be most prolific near the stagnation point

Some regions may be a shear flow

# Electron Timescales in the Intrabinary Shock

- Inverse Compton cooling timescale  $\tau_{IC}$  computed at the stagnation point — Klein-Nishina reductions allow SR cooling to dominate IC cooling at high Lorentz factors



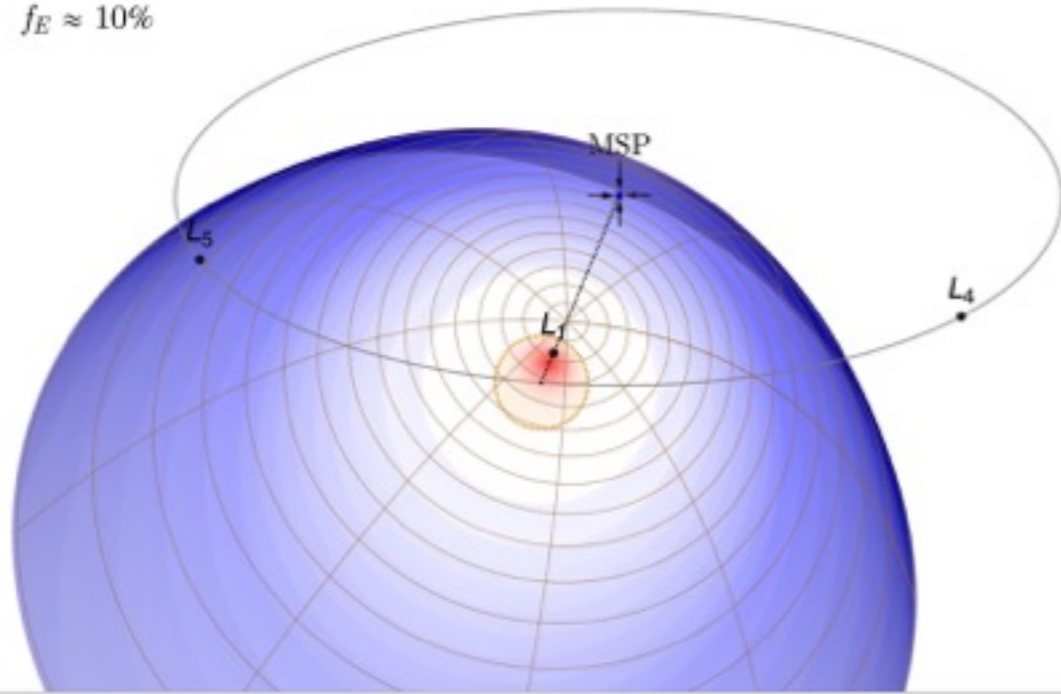
# Orbitally Modulated Doppler Boosting — B1957+20 (*to scale*)

Orbital Phase: -0.03

$R_0 = 0.325$

$i = 65^\circ$

$f_E \approx 10\%$

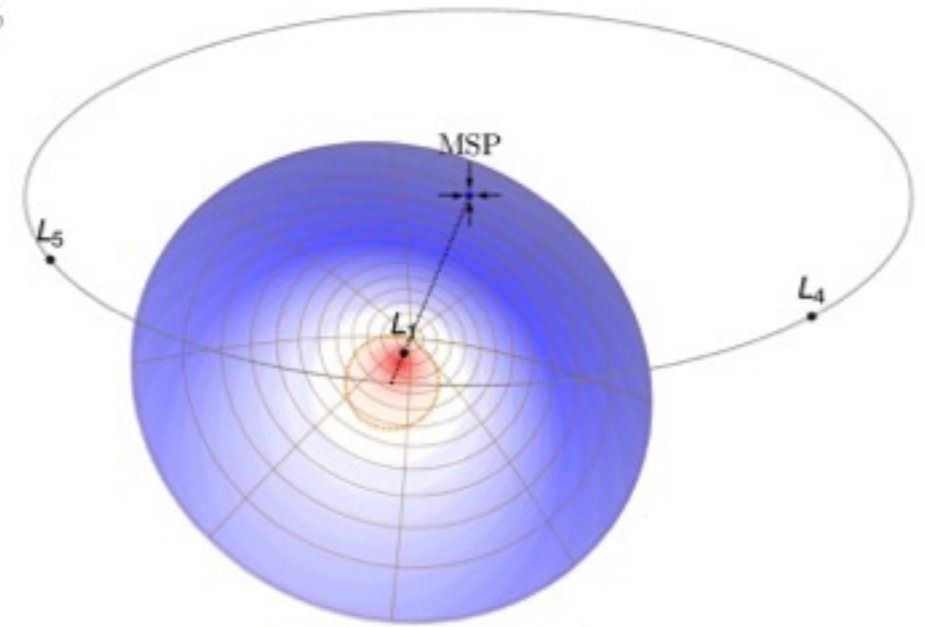


Orbital Phase: -0.03

$R_0 = 0.235$

$i = 65^\circ$

$f_E \approx 10\%$

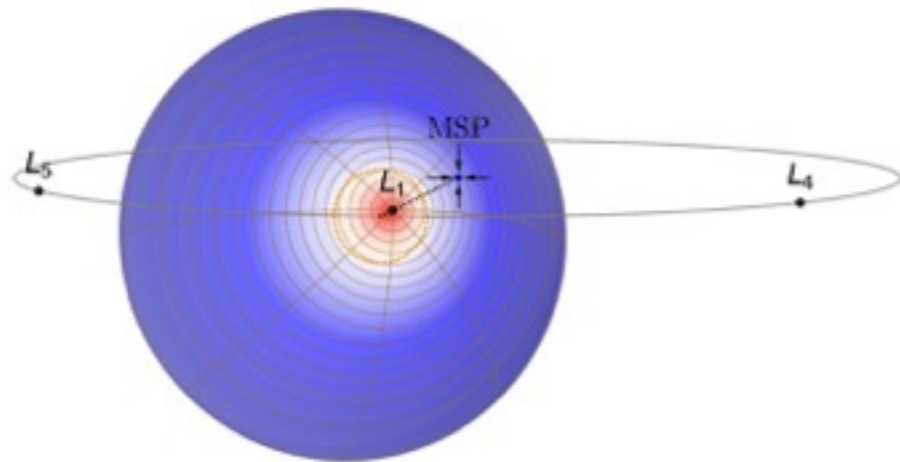


Orbital Phase: -0.03

$R_0 = 0.16$

$i = 85^\circ$

$f_E \approx 10\%$

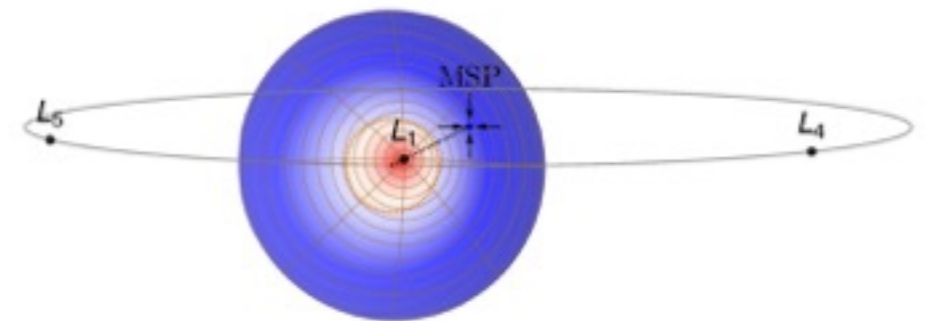


Orbital Phase: -0.03

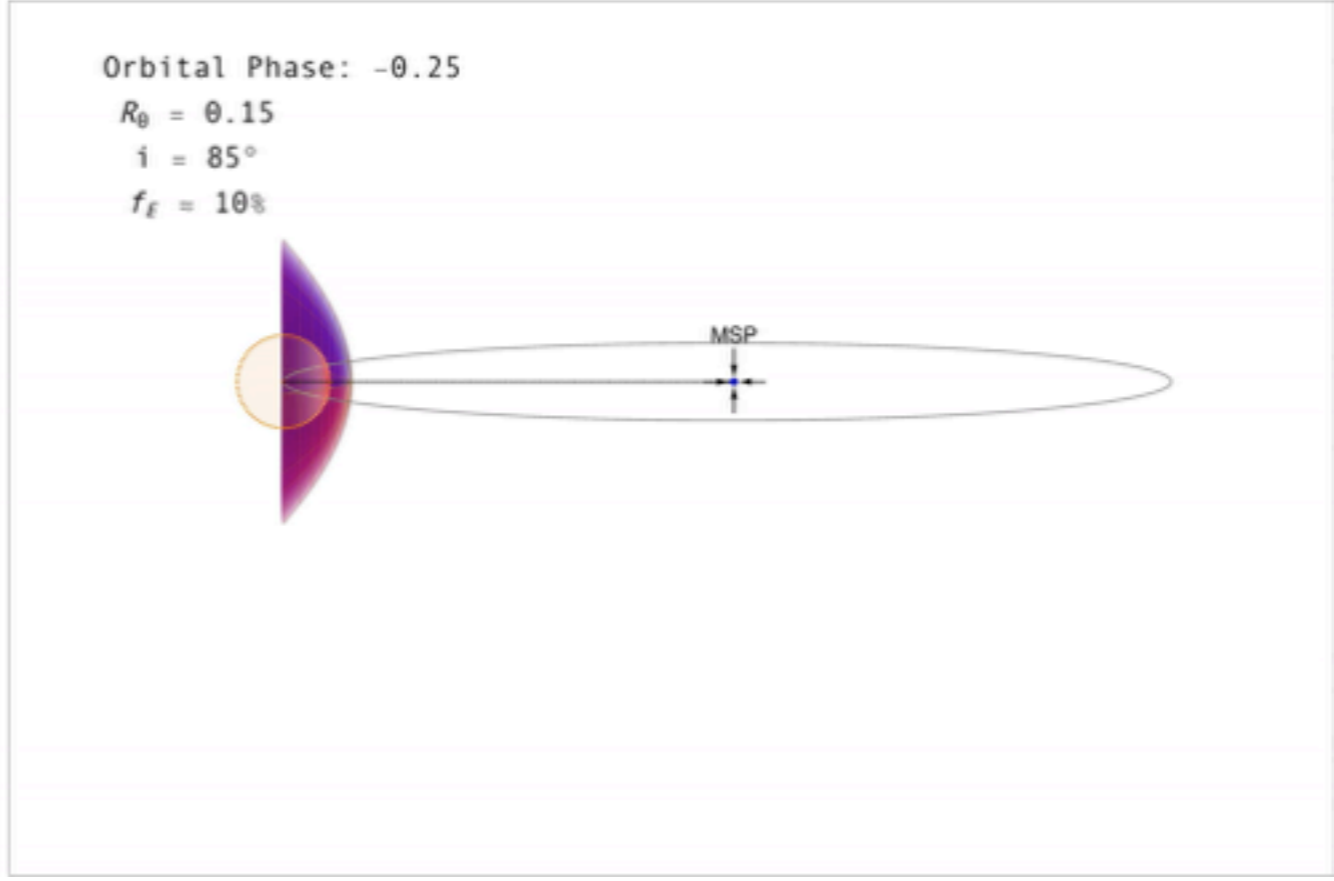
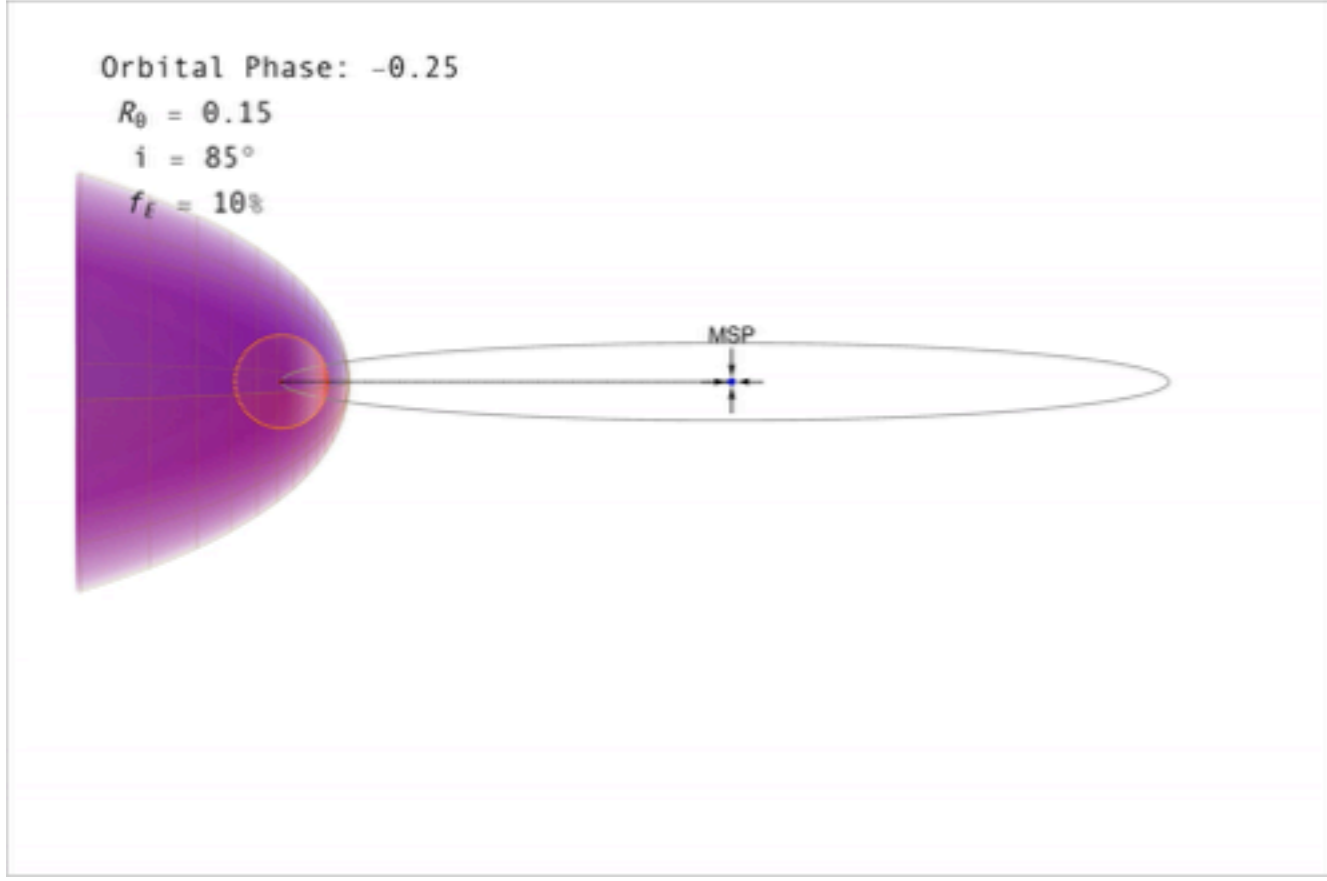
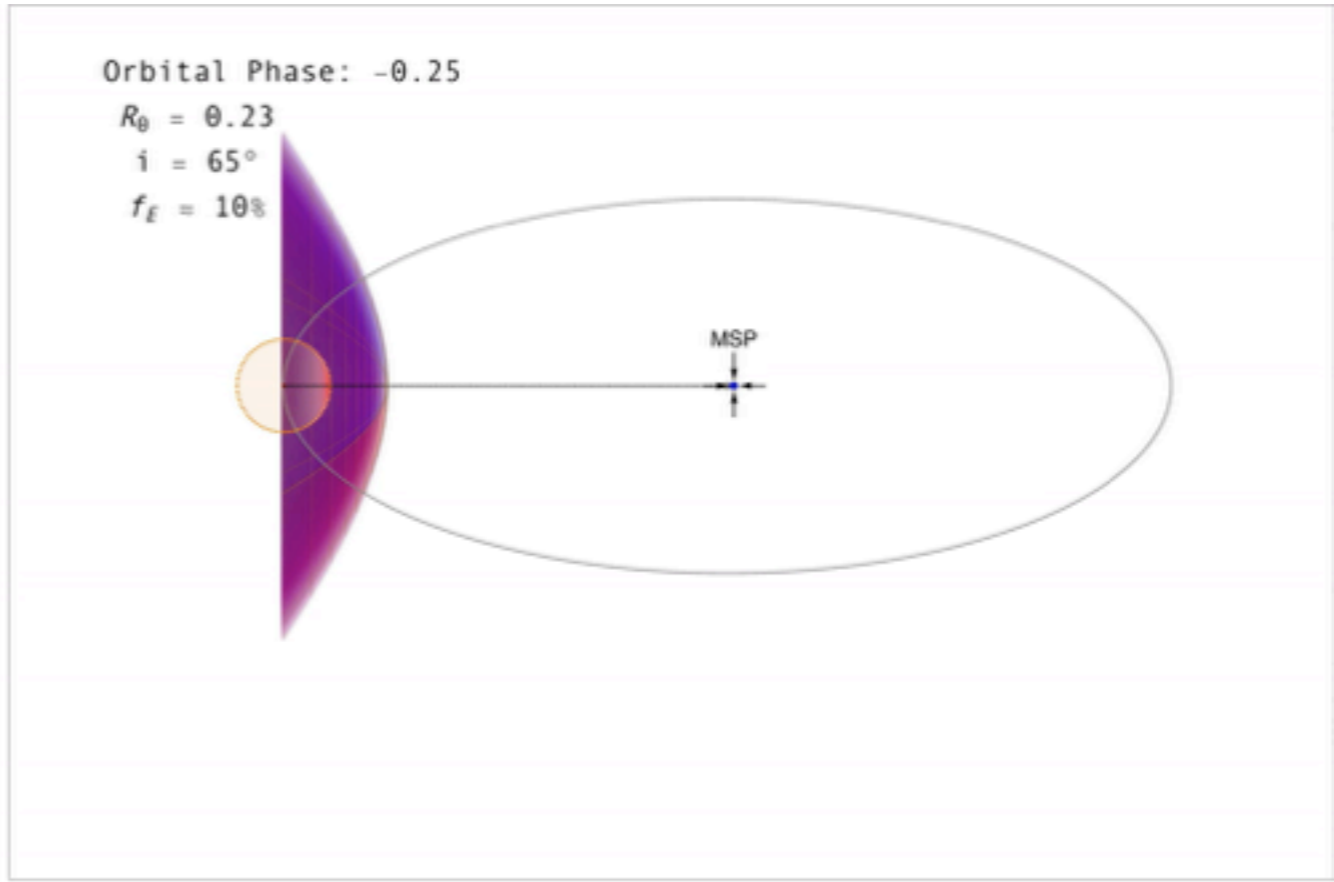
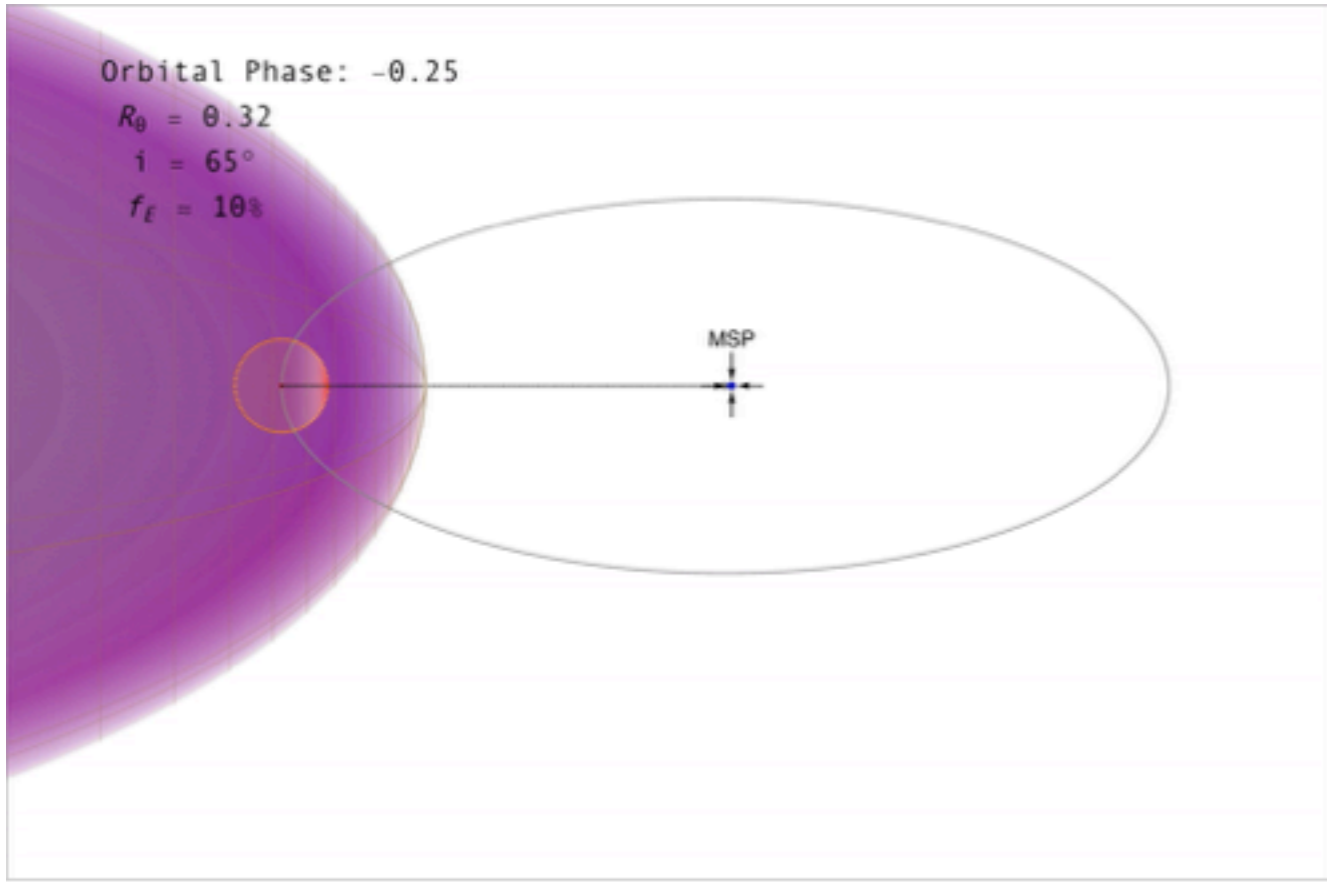
$R_0 = 0.16$

$i = 85^\circ$

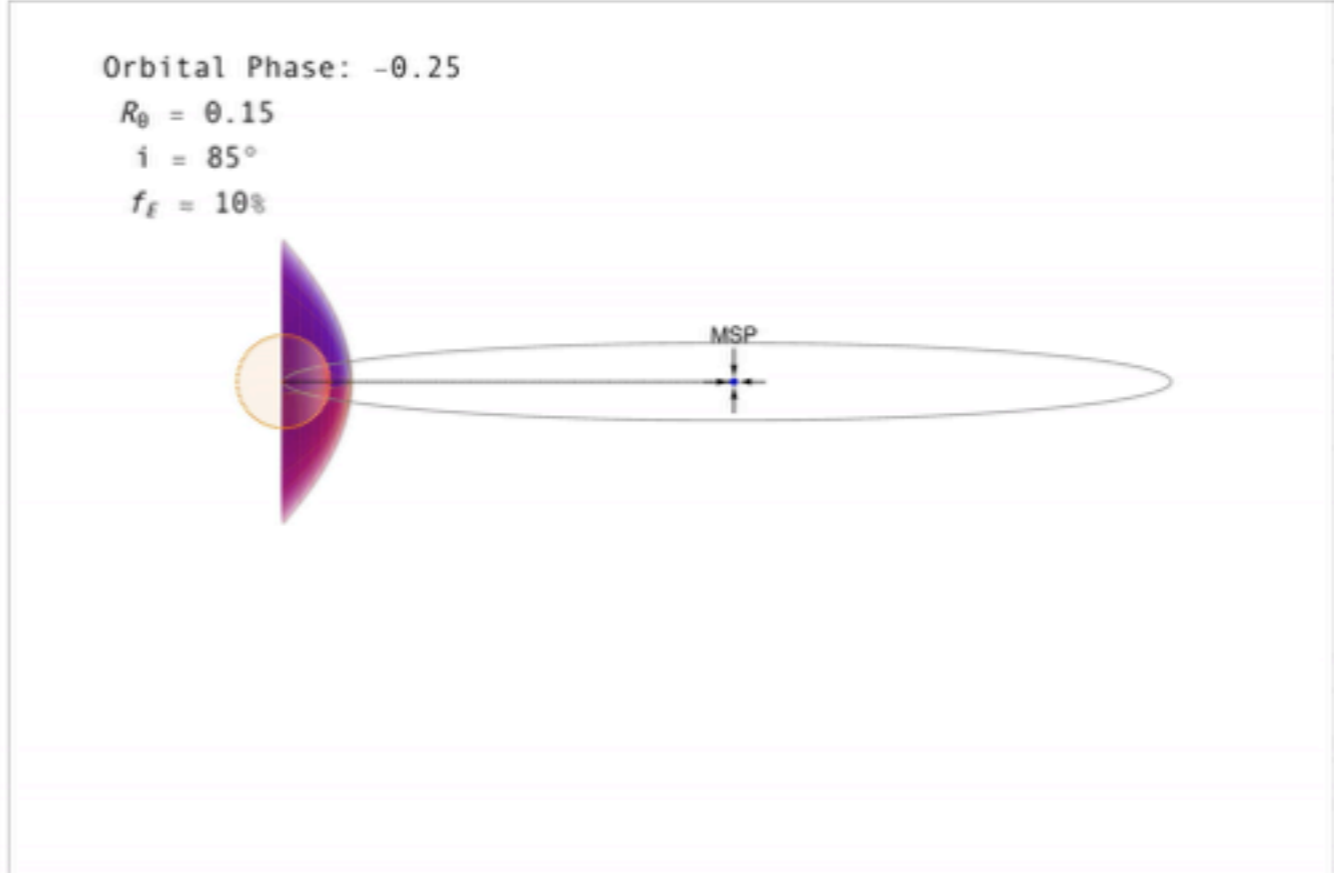
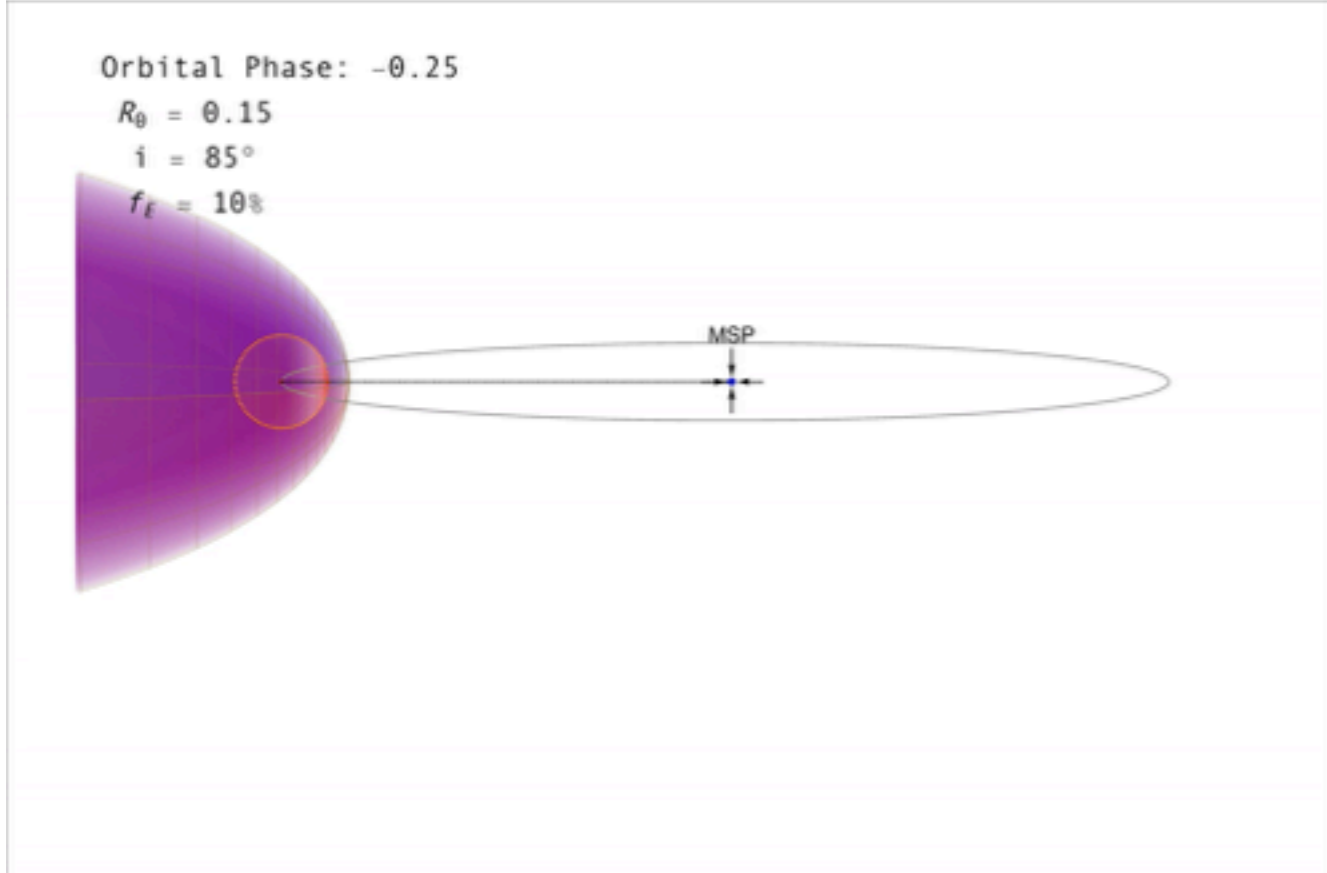
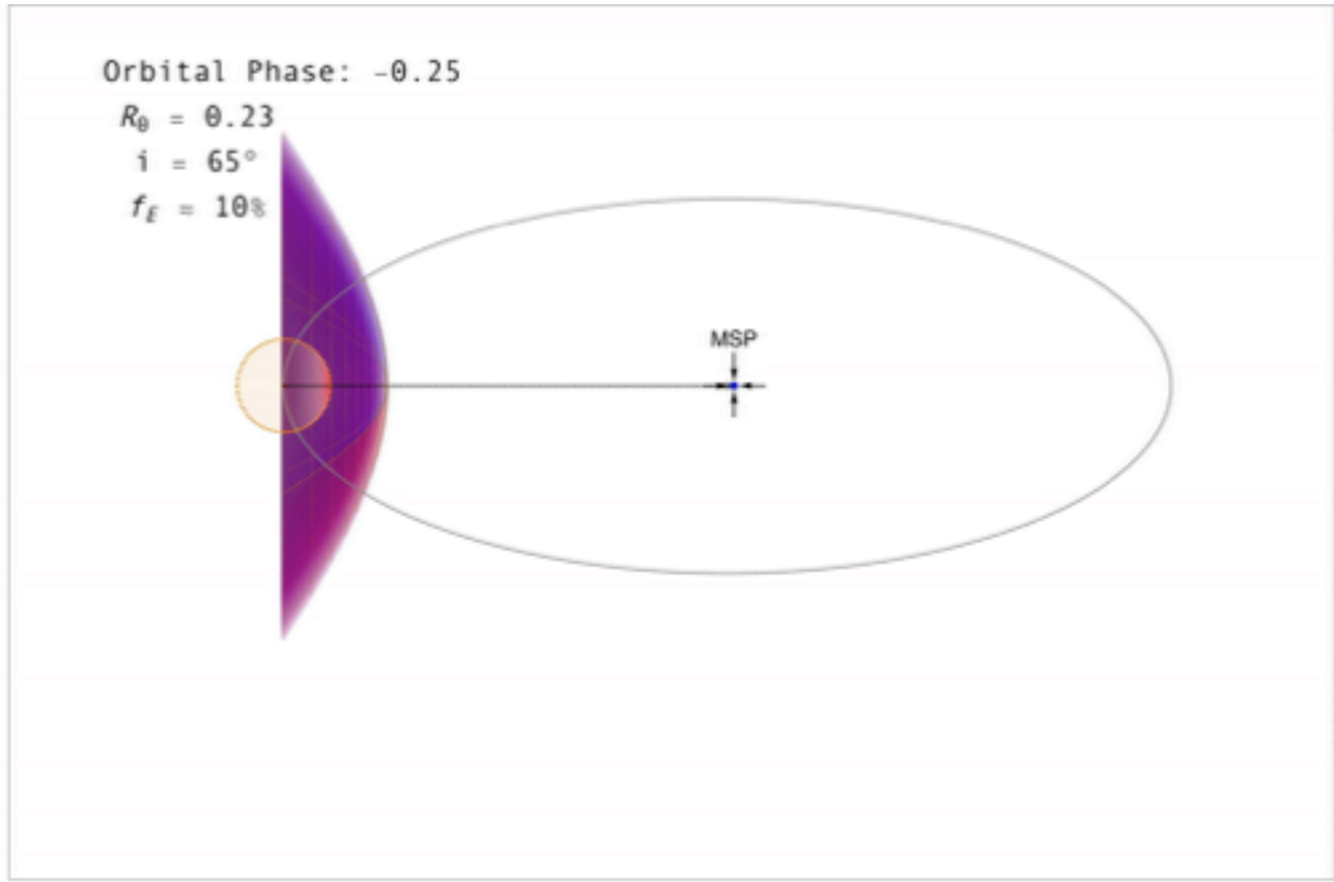
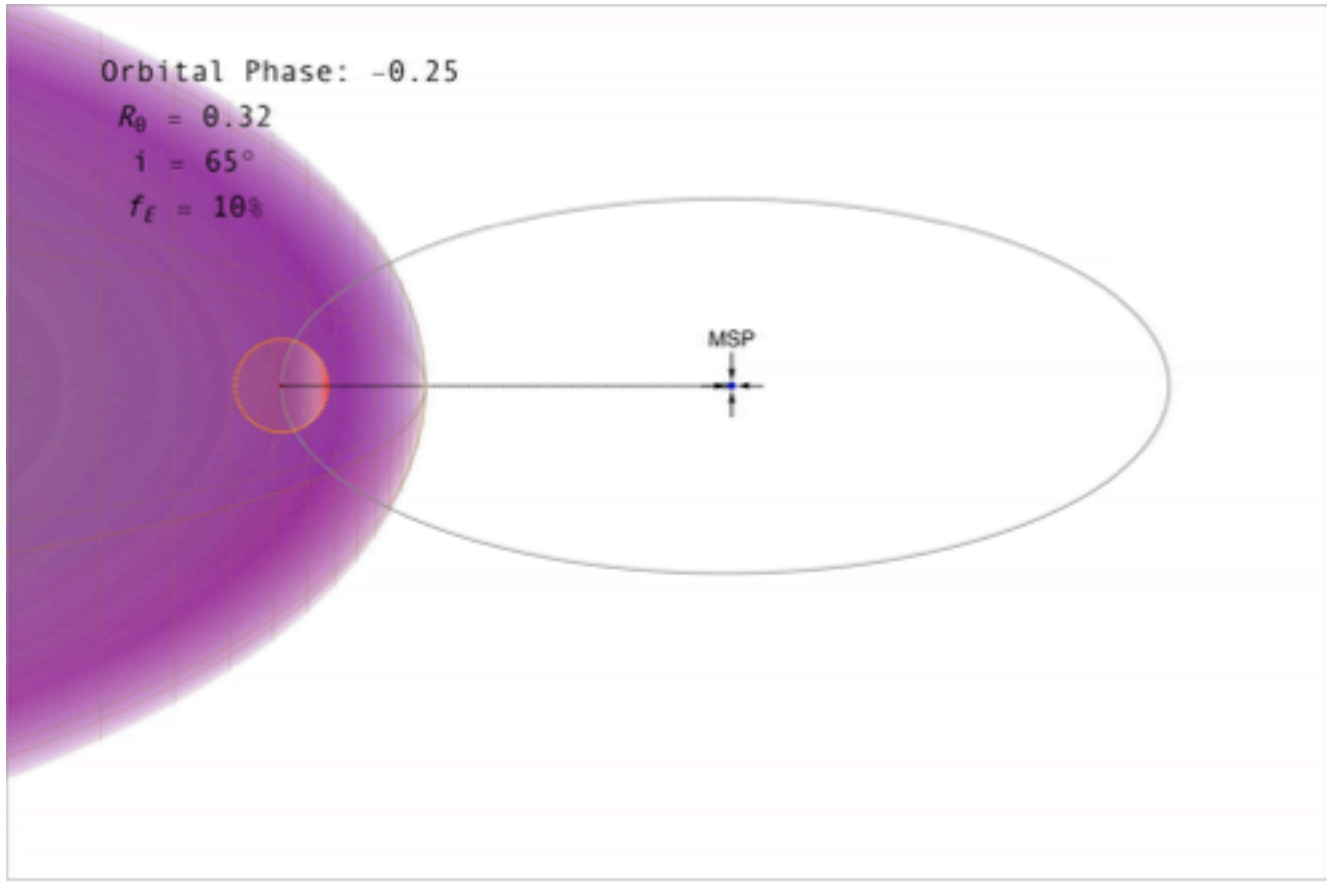
$f_E \approx 10\%$



# Orbitally Modulated Doppler Boosting — B1957+20 (*to scale*)

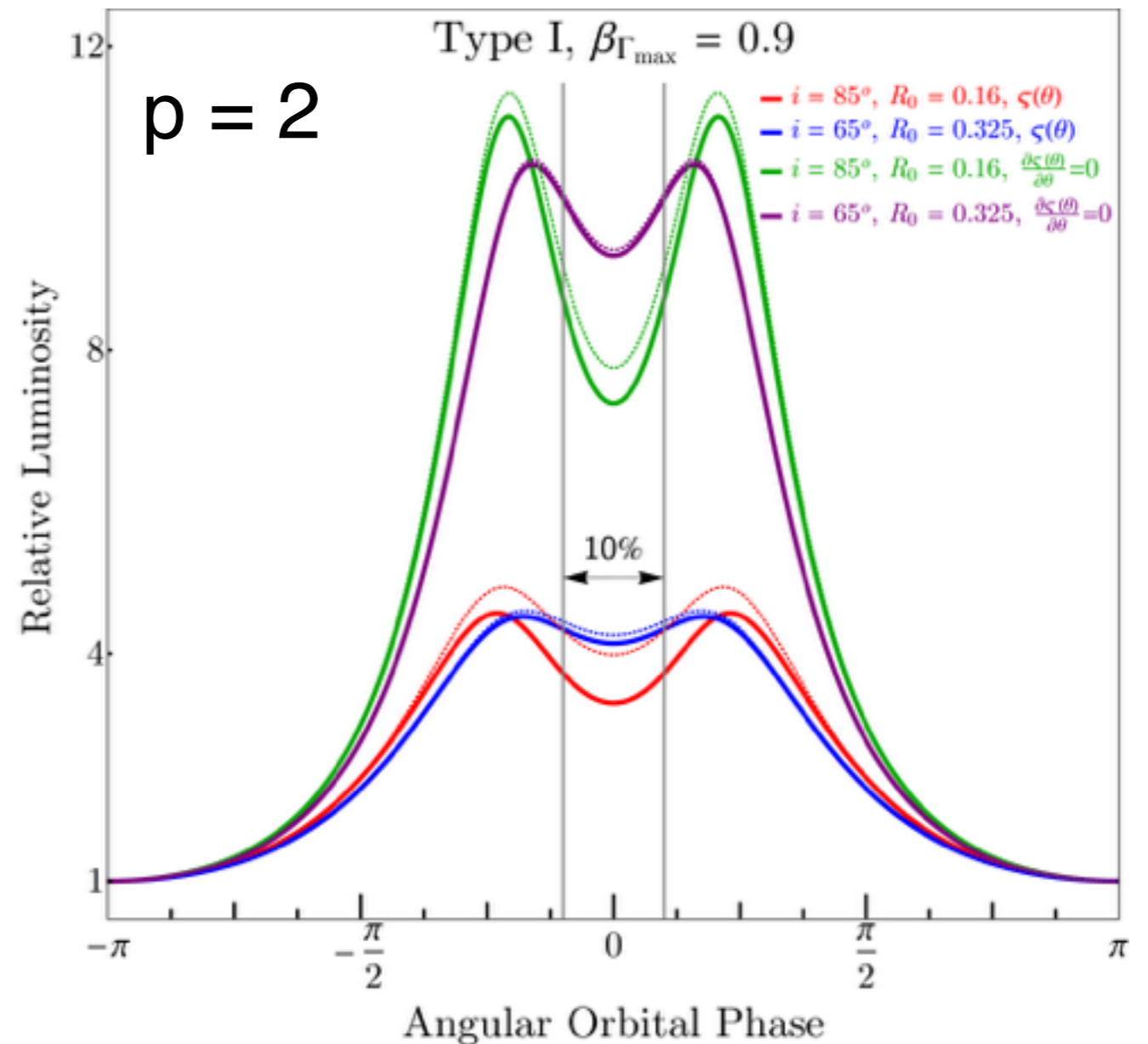
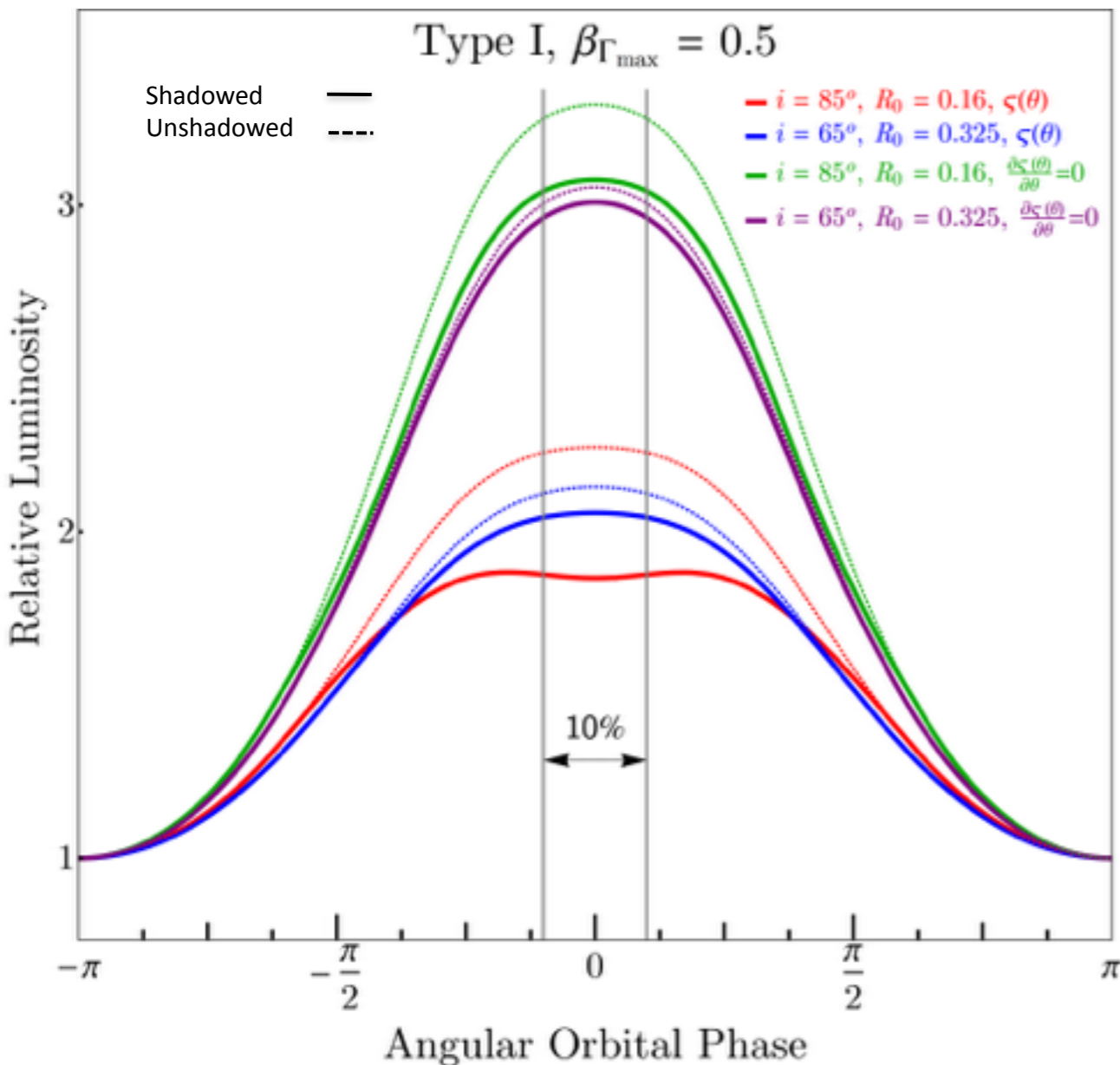


# Orbitally Modulated Doppler Boosting — B1957+20 (*to scale*)



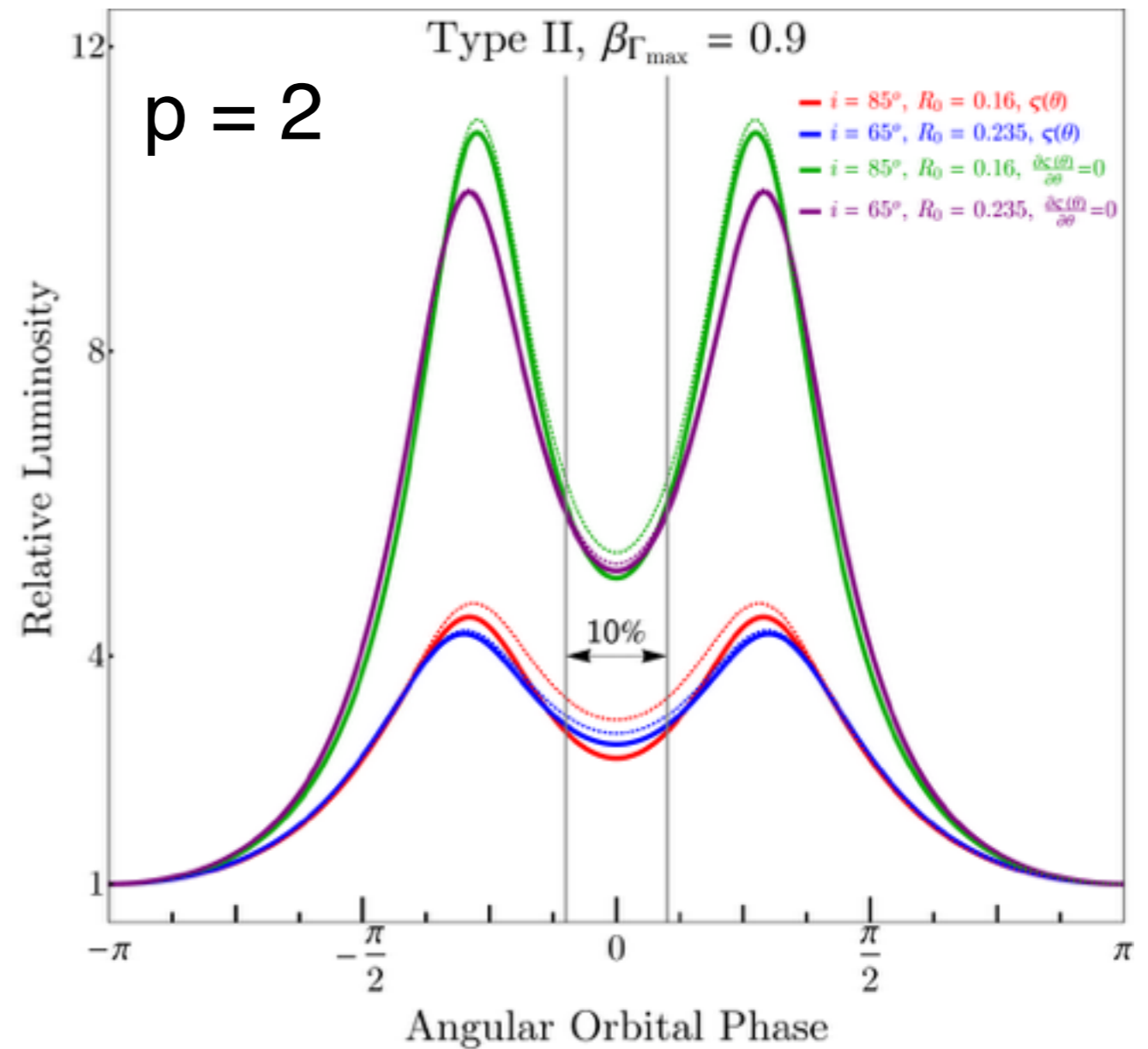
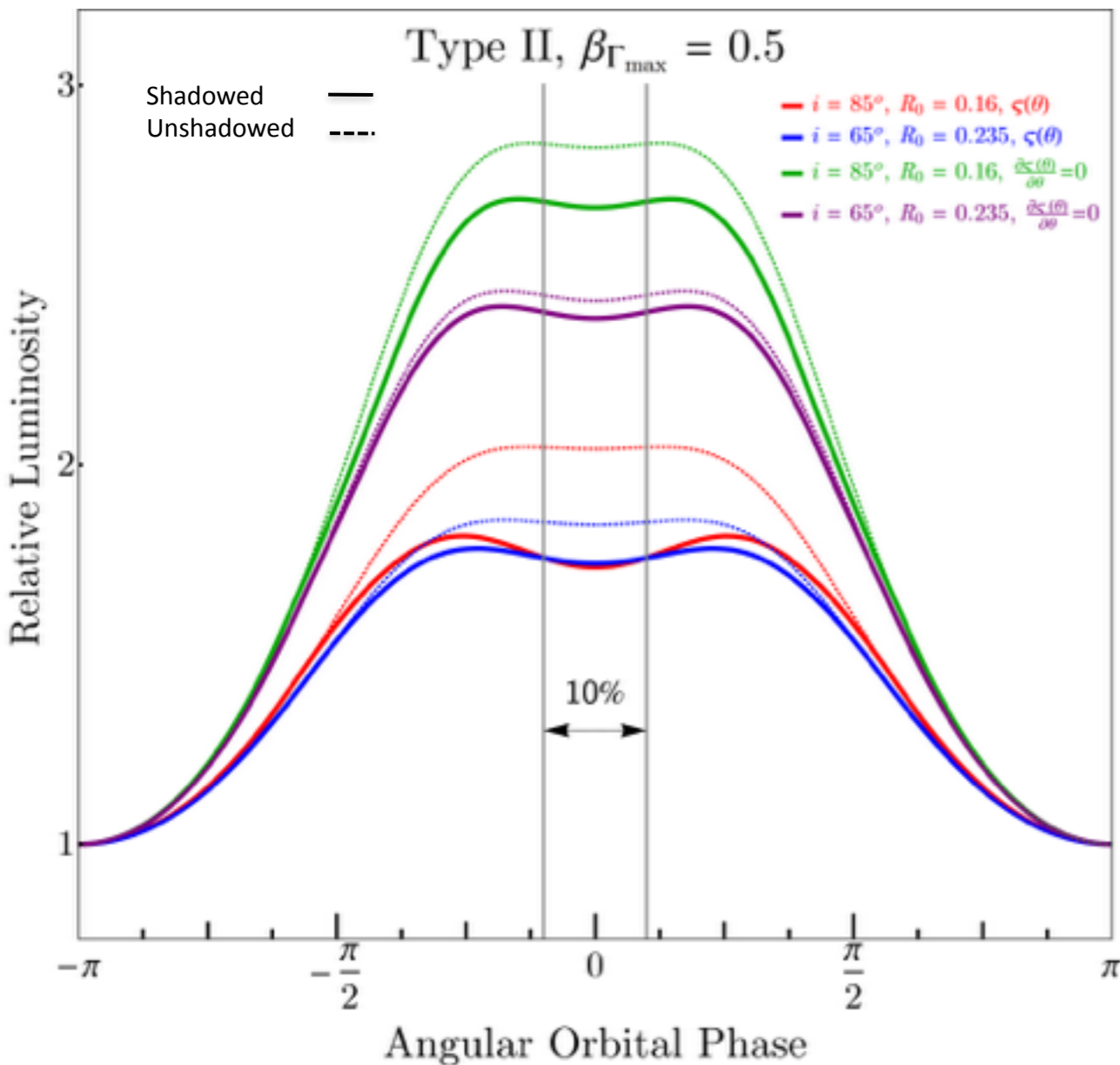
# Orbitally Modulated Synchrotron Emission

- If the bulk velocity along the shock is high enough, doppler boosting produces a characteristic **double-peaked** light curve
- For where the stagnation point  $R_0$  is close to the companion, shadowing can be a strong influence
- **Below:** Orbitally modulated SR emission for B1957+20 at a fixed energy where the emission is a power law, with shadowed and unshadowed fluxes joined and dotted curves, respectively



# Orbitally Modulated Synchrotron Emission

- Complex interplay between the shock shape,  $R_0$ , shadowing, bulk Lorentz factor, and electron density along the shock controls the light curve modulation
- The type II shock scenario yields more significant modulation than the cone-like type I scenario, with a different peak separation for a given inclination



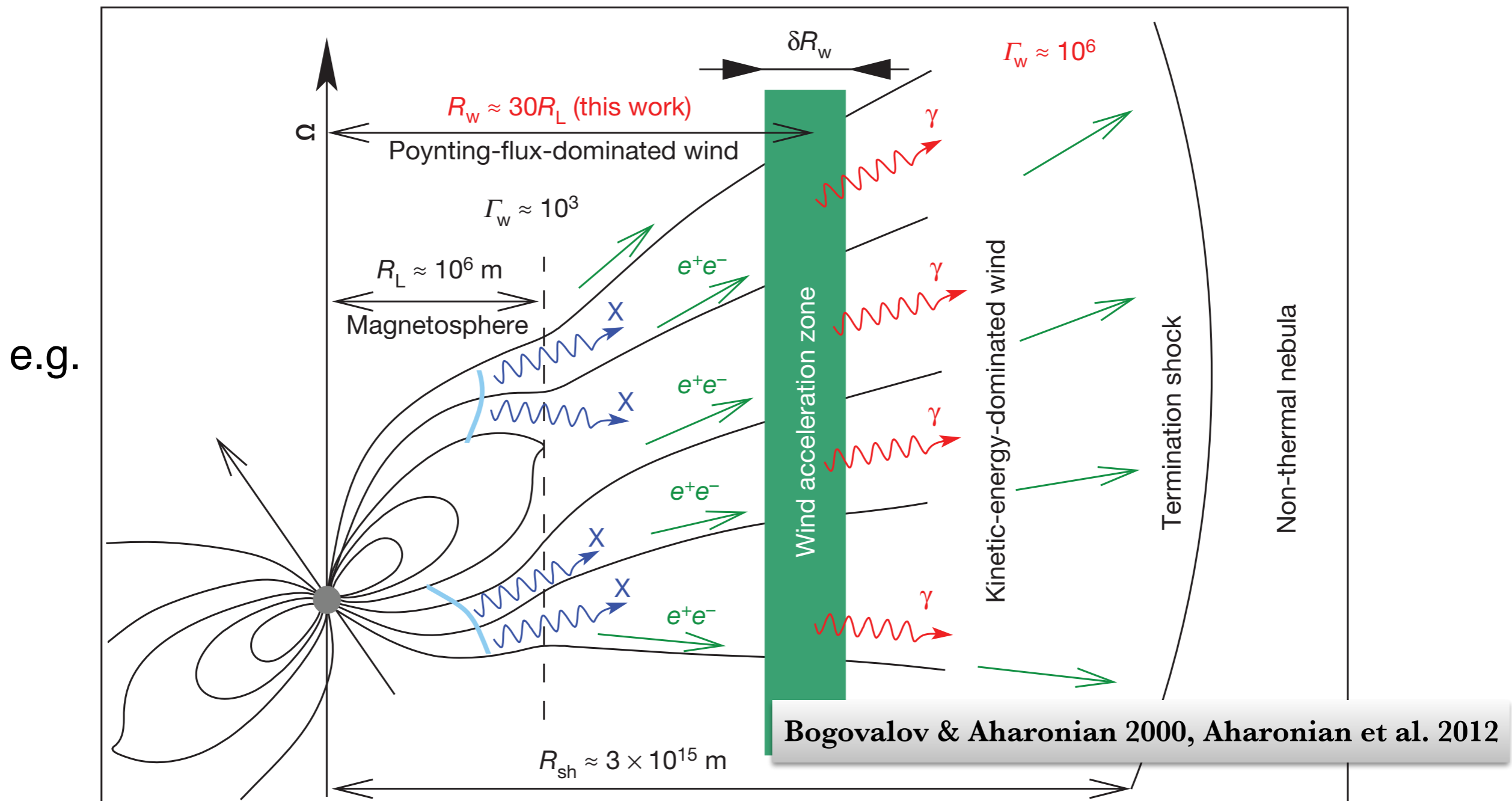
# SR Discussion

- Must originate from the shocked MSP wind (mildly relativistic) rather than the shocked companion wind (nonrelativistic)
- A natural path to produce double-peaked light curves and spectral hardening
- Redbacks where the double peaks are centered around inferior conjunction imply a scenario where **the shock surrounds the pulsar** ==> consistent with >50% radio eclipse fractions (e.g. J1023+0038 in non-accreting state, Archibald et al. 2009) and LMXB state transition
- Optical non-thermal synchrotron emission (and orbitally-modulated *polarization*) could exist depending on the accelerated electron spectrum and level of plasma turbulence in the downstream B
- **Need MeV instrument** to ascertain acceleration efficiency and location of synchrotron peak — ComPair, AdEPT, etc
- Lower second peak possibly due to absorption or asymmetric particle acceleration/transport in the shock induced by orbital motion



# Inverse Compton

- IC target photon fields: companion (optical/UV), shock synchrotron (X-ray), MSP
- Similar physics to TeV binaries, but much more compact
- Accelerated electrons: shock and possibly upstream pulsar wind (e.g. dissipation in the current sheet)

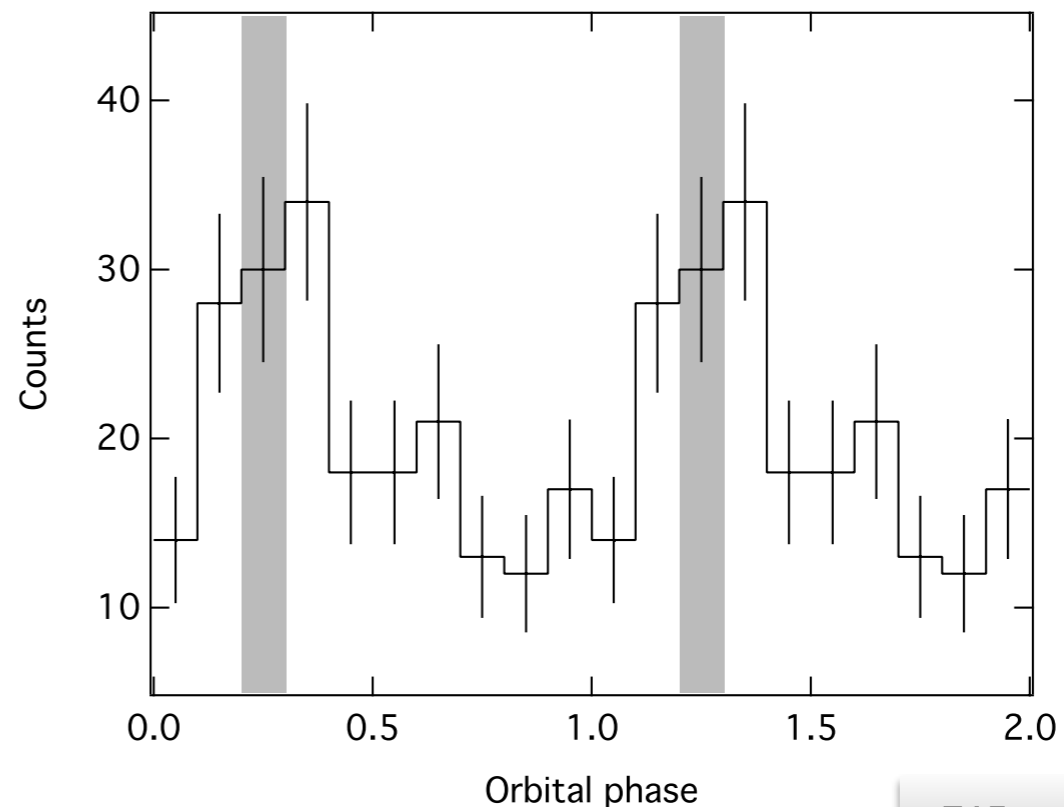
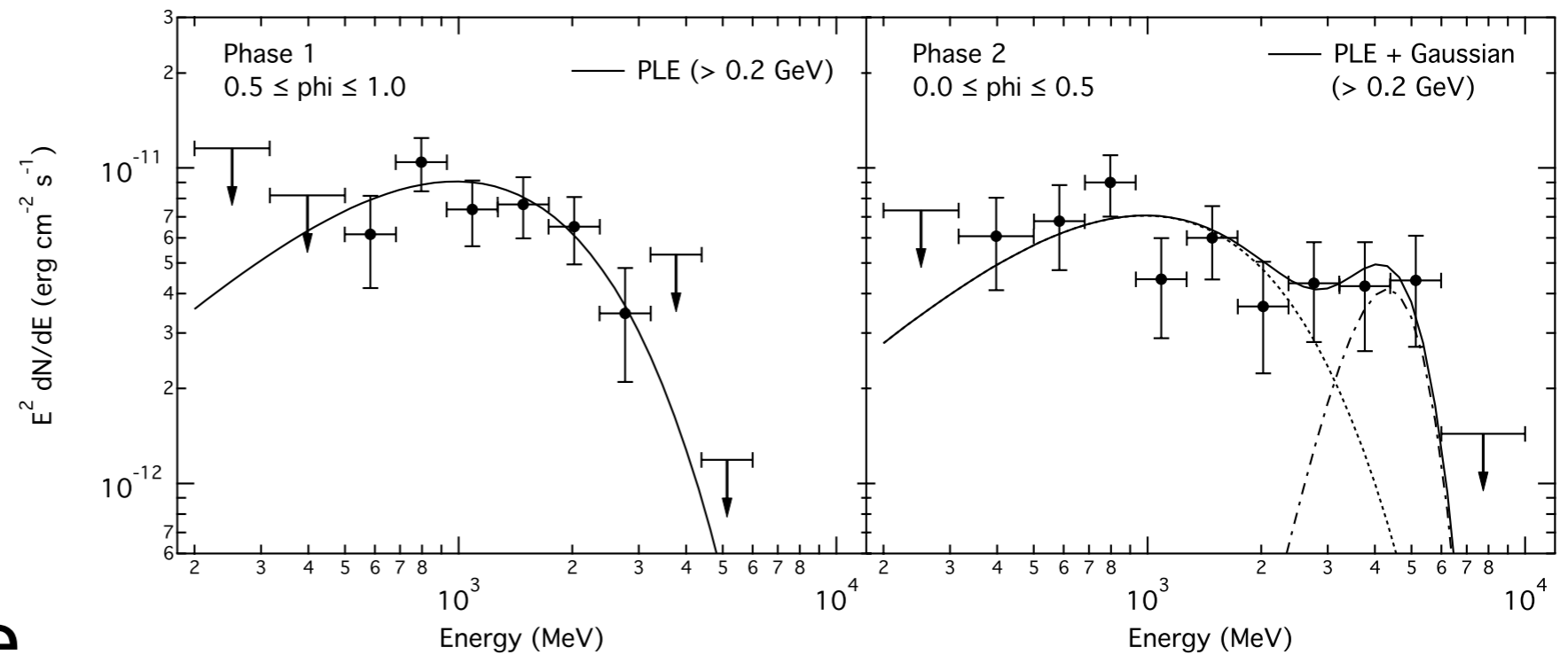


# IC $\gamma$ -ray Observability & Caveats

- Energetics governed by pulsar  $\dot{E}$  & orbital modulation critically dependent on inclination
- Orbitally modulated  $\gamma$ -ray emission has been claimed for B1957+20 (Wu et al. 2012) and J1311-3430 (Xing & Wang 2015) but are unconfirmed (6-10 years, Pass 8 and ToOs to optical flares may help)
- For most systems, the IC optical depth  $< 1$  on orbital lengthscales  $a \sim 10^{11}$  cm, but may exceed unity for hot companions or flaring states where  $T_{\text{hot}} > 10^4$  K
- Optimistically — IC luminosity  $\sim \sigma_T n_\gamma a \times \eta \dot{E} \sim \eta 10^{33}$  erg/s  $\implies \sim \eta 10^{-9}$  ergs/s/cm<sup>2</sup> for  $d=2$  kpc with efficiency  $\eta$  dumped into  $e^+e^-$  and emission is beamed,  $n_\gamma$  should include both thermal and synchrotron photons targets
- Focus should be on nearby systems with high X-ray luminosities, hot companions and flaring states, and near edge-on inclinations

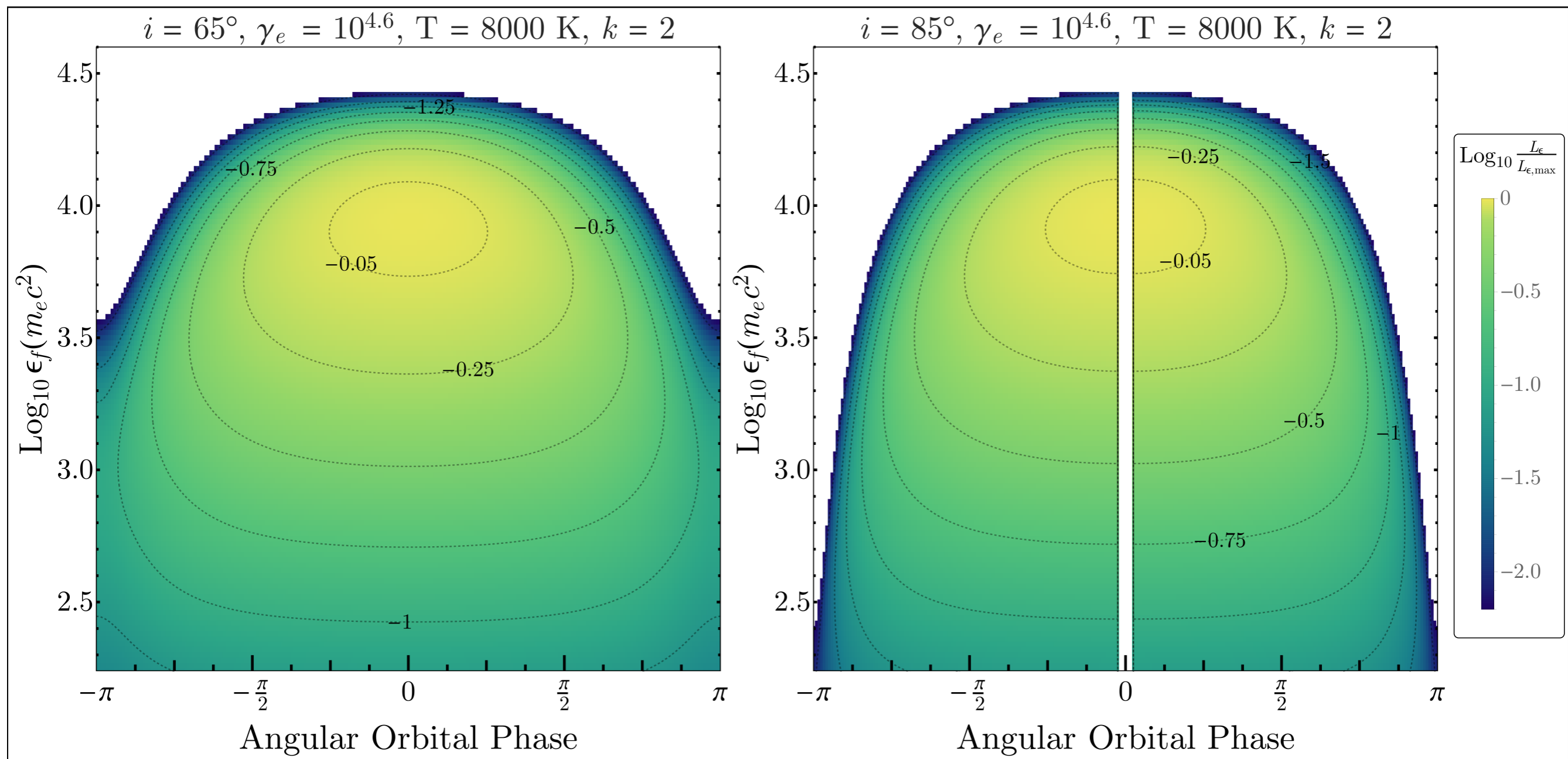
# Inverse Compton - B1957+20

- Only ~ 2-3-sigma significance (post-trials) and unconfirmed by the main collaboration — Pass 8 and 6-10 years of data should confirm or refute



# Orbitally Modulated Cold Wind IC — B1957+20

- Horizontal cuts — light curves; vertical cuts — spectra
- Occultation by the companion of the emission region may be important for inclinations near edge-on
- General agreement with Bednarek (2014)

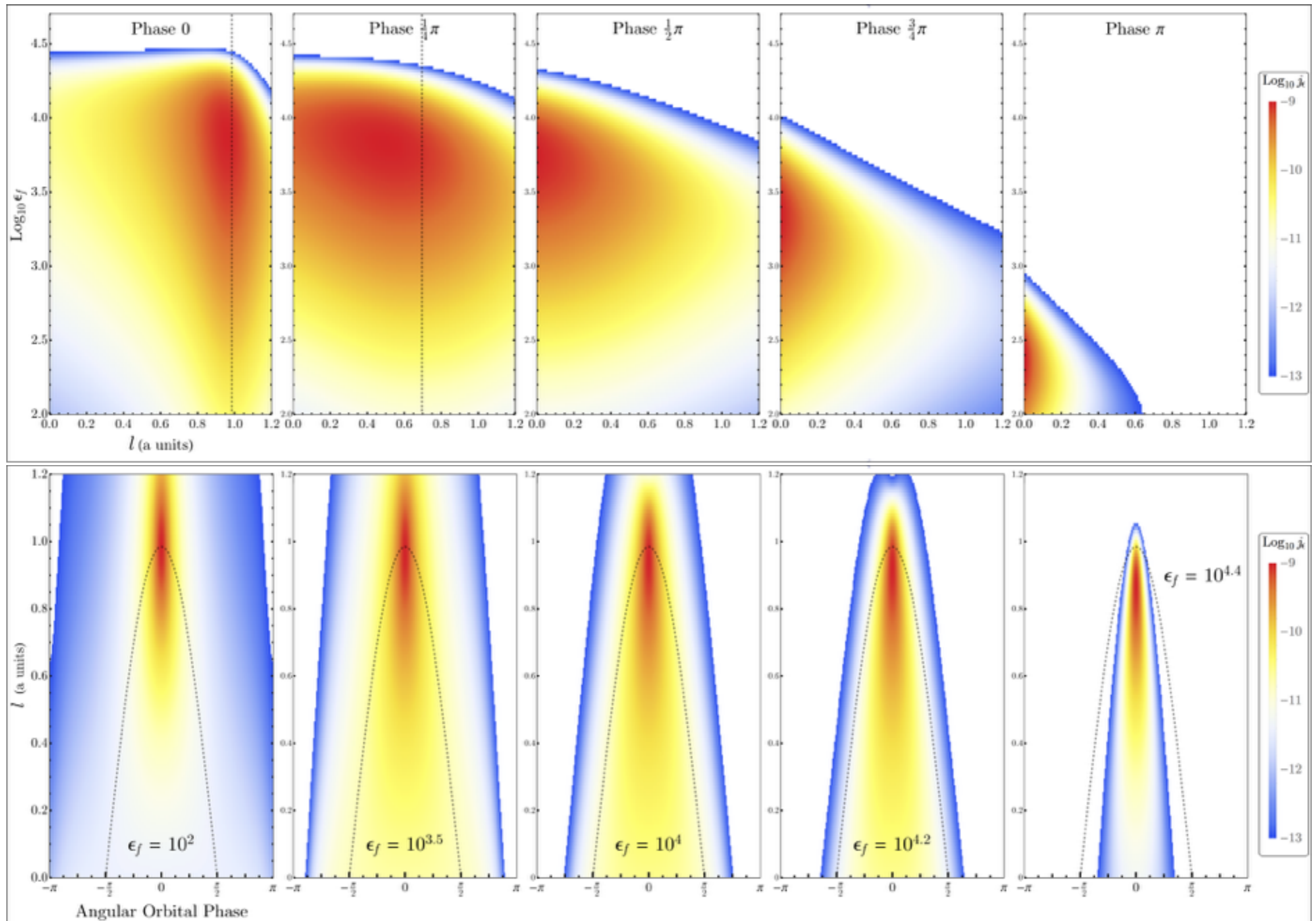


# Future

- Steady-state particle transport along the shock and self-consistent synchrotron light curves
- Additional anisotropic IC components and SEDs
- Relativistic MHD shock structure
- Orbital motion and sweepback effects
- Application of machinery to more eclipsing black widow and redback systems
- Stay tuned!

# Backup Slides

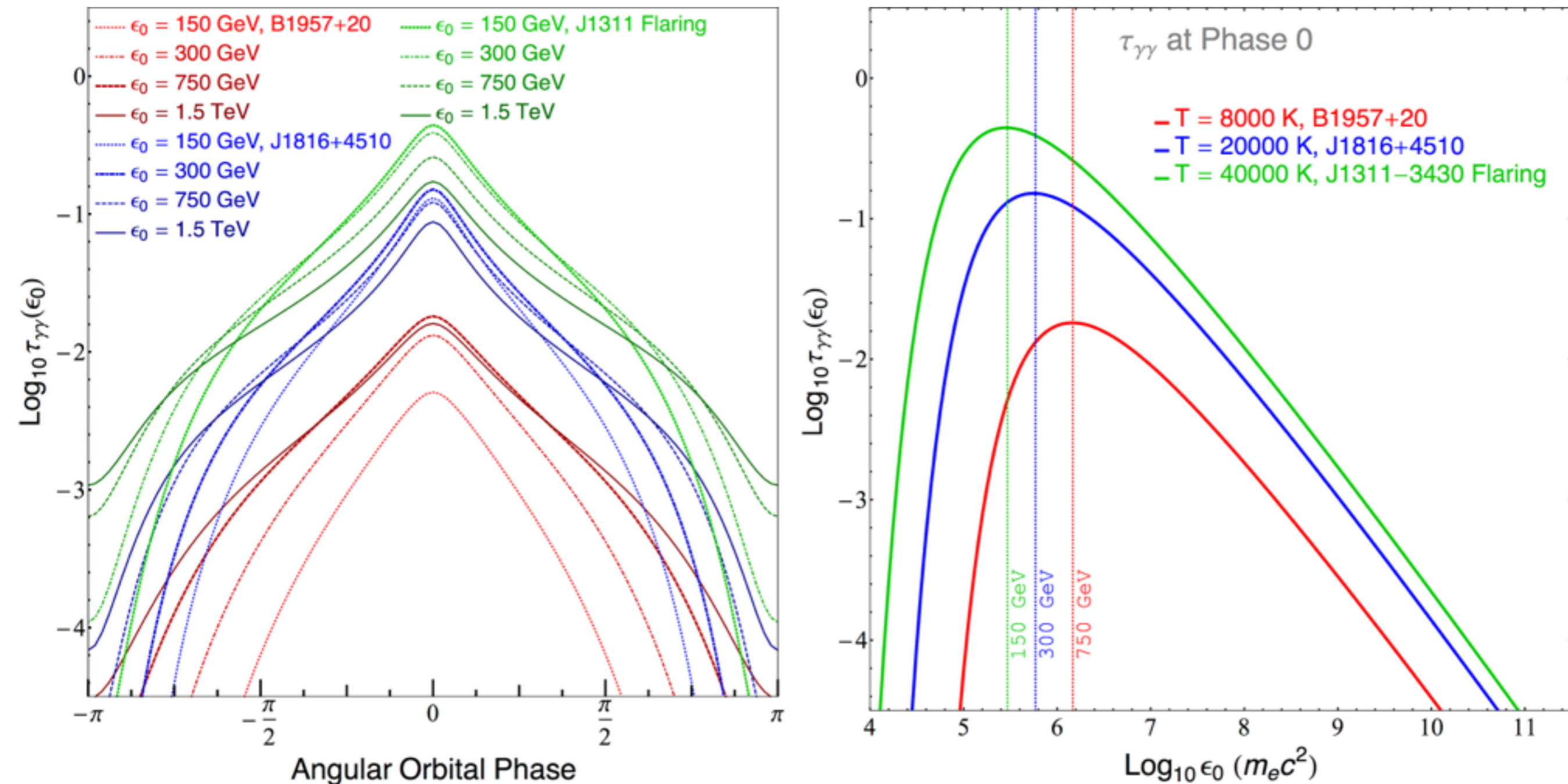
# Volume Normalized IC Emissivity - B1957+20



# $\gamma\gamma$ Absorption & Pair Creation

- Although temperatures of black widow and redback companions can be high, due to their small size, absorption is insignificant except perhaps for J1311-3430 in a flaring state, where  $T_{\text{eff}} \sim 40000$  K
- $\epsilon_0$  - the energy of the outgoing VHE photon, emitted towards observer from  $\sim 0.2a$  near the companion

$$\tau_{\gamma\gamma}(\epsilon_0) = \int_0^\infty d\ell' \int_{\mu_-}^{\mu_+} d\mu_{\gamma\gamma} (1 - \mu_{\gamma\gamma}) \int_{2/[\epsilon_0(1-\mu_{\gamma\gamma})]}^\infty d\epsilon_s \frac{\partial \sigma_{\gamma\gamma}(\epsilon_0, \epsilon_s, \mu_{\gamma\gamma})}{\partial \mu_{\gamma\gamma}} n_\gamma(\epsilon_s) f(\mu_{\gamma\gamma}, \ell')$$





# Growth Curve of Radio Eclipses — Frequency Mapping

- For the eclipses at ingress, the frequency dependence of the eclipse width can give insight into the spatial dependence of the turbulent plasma and absorption causing the eclipses

If the eclipse fraction  $f_E \sim g(\theta) \propto v^{-n}$  with optical depth  $\tau \sim \Sigma \sigma$  and absorption cross section  $\sigma \sim v^{-m}$ , then  $\Sigma(\theta) \sim g(\theta)^{-m/n}$

